An individual-based model for sablefish: Exploring the connectivity between potential spawning and nursery grounds in the Gulf of Alaska

G.A. Gibson[a,*], W.T. Stockhausen[b], K.O. Coyle[c], S. Hinckley[b], C. Parada[d,e], A. J. Hermann[f,g], M. Doyle[b], C. Ladd[g]

[a]*International Arctic Research Center, University of Alaska, Fairbanks, AK 99775-7340, USA*
[b]*Alaska Fisheries Science Center, NOAA/NMFS, 7600 Sand Point Way, NE, Seattle, WA 98115-6349*
[c]*Institute of Marine Science, University of Alaska, Fairbanks, AK 99775, USA*
[d]*Departamento de Geofísica, Universidad de Concepción, Casilla 160-C, Concepción, Chile*
[e]*Instituto Milenio de Oceanografía, Universidad de Concepción, Concepción, Chile*
[f]*Joint Institute for the Study of the Atmosphere and Ocean, University of Washington, Seattle WA 98195*
[g]*Pacific Marine Environmental Laboratory, NOAA, Seattle, WA 98115*

Key words: Sablefish, Recruitment, Modelling, Fish larvae, Gulf of Alaska, Sensitivity analysis

ABSTRACT

Little is known about the mechanism of transport that enables age-0 sablefish (*Anoplopoma fimbria*) to reach suitable nursery sites from spawning locations far offshore, or the strength of the connection between individual spawning sites and nursery areas, or how variability in the strength of these connections may impact recruitment success. Using a model for the early life stages of sablefish, we explored the variability in connectivity between spawning and recruitment sites that can arise solely from interannual variability in environmental forcing and its impact on transport. Our major findings are that 1) the model indicates young sablefish settling in nursery areas in the Gulf of Alaska were most likely spawned in the eastern Gulf; 2) sablefish spawned in the western Gulf of Alaska are unlikely to settle anywhere in the Gulf, and are more likely to be advected farther west, perhaps to settle in the Aleutian islands or Bering Sea (to contribute to the Alaska population, they would have to undergo an active return migration as they mature); 3) total connectivity between all spawning sites and nursery areas showed stronger correlation with recruitment estimates than the strength of connections to or from specific regions; and 4) transport to St. John Baptist Bay, a known sablefish nursery area, was not the most probable end point for sablefish spawned throughout our Gulf of Alaska model domain. This suggests that young individuals arrive at this persistent nursery area due to directional swimming behavior, highly localized spawning, or small-scale currents not captured in the hydrographic model. The fact that no single correlate in our analysis had a very strong relationship to sablefish recruitment indicates that recruitment variability arises from complex interactions between the environment and the individual, and a possible disconnect in spatial scales between the Gulf of Alaska sablefish IBM and the broader sablefish stock assessment, which includes both the GOA and the Eastern Bering Sea, as well as possible contributions from

/

Canadian stocks to the south. Our analyses determined that although the timing and extent of this transport shows significant interannual variability, both the location of likely sablefish spawning (source) areas and the comparative strength of connectivity between spawning and nursery sites appear to be relatively consistent year-to-year.

*Corresponding author. Phone: 907 474-2768. Fax: 907-474-5662.

E-mail address: ggibson@iarc.uaf.edu (G.A. Gibson)

1. Introduction

Because the recruitment of individuals to juvenile and adult marine fish stocks is an important process driving population fluctuations, understanding recruitment processes can inform sustainable fishery management and ecosystem planning. In this context, “recruitment” refers to the annual abundance of individuals entering a specific population classification (e.g. age-2, or “fishable”). Unfortunately, variability in recruitment is poorly understood for many populations, though it is thought to be at least partially controlled by physical (i.e. climate and transport) and biological (i.e. growth and predation) processes affecting the survival of early life stages (eggs, larvae, juveniles). Achieving an understanding of the factors affecting recruitment variability in the relatively productive Gulf of Alaska (GOA) region is made more difficult by the complexity of the physical and biological systems. Strong currents, complicated topography, and highly variable freshwater runoff contribute to a dynamic and complex physical system, which in turn influences the entire ecosystem. The Gulf of Alaska Integrated Ecosystem Research Program (GOAIERP, Dickson and Baker, 2016) was designed to identify how environmental variability in the region affects the recruitment of five commercially and ecologically important groundfish species: Pacific cod (*Gadus macrocephalus*), walleye pollock (*Gadus chalcogramma*), Pacific ocean perch (*Sebastes alutus*), sablefish (*Anaplopoma fimbria*), and arrowtooth flounder (*Atheresthes stomias*). The central hypothesis of the GOAIERP program was that early life survival is the primary factor determining the year-class strength of these species in the GOA. Success in navigating the "gauntlet"—that is, the challenges these fish face during their first year of life, as they attempt to travel from spawning areas to “settlement” in young-of-the-year nursery sites—is key. This gauntlet may be impacted by physical factors such as water temperature, substrate type, and the strength and direction of currents, as well as biological factors such as food availability and predator abundance.

To assess the impact of environmental variability in driving the transport and success of early life stages from spawning to settlement, in addition to a comprehensive field program, GOAIERP included a modeling component that integrated a suite of oceanographic, lower trophic level, and individual-based fish modeling tools. By providing a broader spatial and temporal reference framework than it was possible for the field program to achieve, the GOAIERP modeling effort aided in the interpretation of observations, identification of knowledge gaps, and evaluation of the relative importance of recruitment mechanisms. This present study discusses the results of our individual-based sablefish modeling study. Little is known about the mechanisms of transport that enable age-0 sablefish to reach suitable nursery sites from spawning locations far offshore, the strengths of the connections between individual

spawning sites and nursery areas, or how variability in the strengths of these connections may impact recruitment success. Using a biophysical, individual-based model (IBM) for the early life stages of sablefish, we addressed the variability in connectivity between spawning and early juvenile nursery sites that can arise solely from interannual variability in environmental forcing and its impacts on transport.

Sablefish, more commonly known as black cod, have long been considered a delicacy, and represent a highly valued commercial species (Fissel et al., 2012; King et al., 2001). The sablefish fishery is located around the North Pacific Rim - as far west as the Japanese coast, up to Cape Navarin in the northern Bering Sea, throughout the Aleutian Islands and the GOA, and as far south as Baja California (Hart, 1973; Kodolov, 1968; Sasaki, 1985; Wolotira et al., 1993). Most of the catch comes from Alaskan waters (Heifetz and Fujioka, 1991), with the largest concentrations of sablefish in the GOA found in the central and eastern Gulf (Hanselman et al., 2014b; Table 3), corresponding with their principal spawning grounds (Funk and Bracken, 1984). Adult sablefish are semi-demersal and have been observed within 1 m of the sea floor (Krieger, 1997) in deep waters on the outer shelf and the continental slope, and in coastal fjords at depths of 200-1000 m (Allen and Smith, 1988; Kendall and Matarese, 1987; Mason et al., 1983; McFarlane and Beamish, 1983), though most fish have been observed between 300 and 700-m depths (Maloney and Sigler, 2008). Due to their commercial value, sablefish populations have been the target of fisheries since the end of the 19th century (McDevitt, 1986; Sasaki, 1985). In 2014, the sablefish ex-vessel price of $4.15/lb was below its peak of $5.85/lb in 2011, but above the $3.91/lb ten-year average (NMFS, 2014). As such, it remains one of the most lucrative of Alaska fisheries, and even small changes to the annual catch would result in significant changes to the total value of the catch. Reliable estimation of year-class strength, a key component of the stock assessment process, is hindered by limited knowledge of early life history stages, as well as the underlying environmental processes influencing survival prior to recruitment to the fisheries (Shotwell et al., 2014).

Age at 50 % maturity is between 5-7 years for sablefish (Mason et al., 1983; Head et al., 2014). After reaching maturity, sablefish move into offshore areas over the continental slope where female sablefish spawn pelagic eggs at depths of 300 m or more (Mason et al., 1983; Moser et al., 1994), with a majority of actively spawning females actually observed at depths greater than 800 m (Hunter et al., 1989). Sablefish are highly fecund, with an average-size spawning female (65-75 cm) producing 180-280 thousand eggs annually, and larger females (90-100 cm) producing up to one million eggs (King et al., 2001). Sablefish release eggs in three to four batches (Hunter et al., 1989; Kimura et al., 1998; Macewicz and Hunter, 1994) between January and May throughout their range, perhaps with an exception of those above 55°N in the Bering Sea, where low temperatures may inhibit this process (OCSEAP, 1986). Otolith analysis suggests that in the GOA the average spawning date is March 30 (Sigler et al., 2001), though peak spawning occurs in February (Doyle and Mier, 2015; Hanselman et al., 2014b). Mason et al. (1983) interpreted an absence of eggs above 400-500 m in later stages of development, coupled with a preponderance of newly hatched larvae, as evidence of egg descent into deeper waters prior to hatching at depth. Similarly, a study of sablefish egg density suggests that, while eggs rise initially after spawning, they then sink prior to, and during, hatch. Larvae do not exhibit spontaneous movement until approximately twenty days after initial fertilization of the egg (Alderdice et al., 1988), at which time they can actively swim toward the surface and join the neuston. Young sablefish exhibit short diel migrations (Sogard and Olla, 2001) as they continue to develop in the upper water column. Young sablefish have been observed as far offshore as

160 km in southeast Alaska (Wing and Kamikawa, 1995) and 240 km in the Aleutians (Kendall and Matarese, 1987) but by the end of the first summer, the young-of-the-year (YOY) have arrived in the inshore environment, where they spend at least the winter and following summer in coastal bays and inlets (Maloney and Sigler, 2008; Mason et al., 1983; Rutecki and Varosi, 1997). Opportunistic surveys performed in nearshore bays and inlets throughout southeast Alaska suggest that YOY sablefish occur consistently in only a few locations such as St. John Baptist Bay (Fig. 1, Rutecki and Varosi, 1997)—while in cases of year-classes associated with high recruitment, age-1 juveniles are abundant at nursery sites throughout the continental shelf of the GOA. It is thought that such a widespread presence over the shelf is indicative of a strong year-class (Hanselman et al., 2014b). This suggests that while YOY sablefish may utilize a variety of benthic habitats in the nearshore, the specific features of a few locations may be unique or especially beneficial to survival, and thus critical to maintaining a base level of recruitment.

As sablefish do not exhibit spontaneous movement until almost nineteen days after hatching (Alderdice et al., 1988), sablefish eggs and young juveniles can be considered planktonic, with little ability to swim against the current, and thus are likely dependent on the prevailing circulation pattern for transport to suitable inshore nursery sites. In the northern (>59°N) GOA, circulation is predominantly east to west. The Alaskan Stream is a westward flowing boundary current with flow rates up to 80-100 cm s^{-1} along the continental shelf break (Reed, 1984). On the shelf, within about 50 km of the coast, the Alaska Coastal Current is a westward-flowing, buoyancy-driven current (Royer, 1998; Stabeno et al., 2004), with maximum daily flow rate of 26-117 cm s^{-1} (Stabeno et al., 1995). In the eastern GOA (<140°W), the wide and variable Alaska Current flows northward along the shelf break, while the Alaska Coastal Current flows northward along the shelf. The narrowness of the shelf in the eastern GOA results in strong interaction between the shelf-break flow and the coastal current (Stabeno et al., 2016). Both the shelf break currents and the coastal current can meander and shed eddies, affecting the trajectories and mixing of water masses (Bailey et al., 1997; Janout et al., 2009; Ladd and Stabeno, 2009; Ladd et al., 2005; Okkonen, 2003). Storms generated by the Aleutian Low atmospheric pressure system promote onshore advection of surface waters (Cooney, 1986), and the coastal mountain range constrains these pressure systems resulting in elevated precipitation and runoff (Royer, 1982). Variation in the storms and runoff result in interannual variability in the strength of the circulation and onshore advection. It has been speculated that success of YOY sablefish is related to advantageous currents advecting young sablefish to suitable nursery sites, and to the presence of sufficient food availability to support their rapid growth (Kendall and Matarese, 1987; McFarlane and Beamish, 1992; Sigler et al., 2001). Individuals that are not transported to suitable nursery areas within the critical time frame presumably succumb to a lack of food or shelter, and subsequently die (Coutré et al., 2015).

Sablefish recruitment appears to be characterized by long periods of relatively low levels between very strong year-classes (Funk and Bracken, 1984). In the annual assessment for sablefish stock in Alaska, which treats sablefish in both the GOA and the eastern Bering Sea as a single stock, recruitment is defined as the number of age-2 sablefish entering the assessment model (Hanselman et al., 2014b). For a typical marine fish stock, the two primary factors affecting recruitment are the level of adult spawning and the ecological processes influencing egg-to-recruit survival. For sablefish, the level of adult spawners seems to be a secondary factor (Hanselman et al., 2014b), as spawning success appears to be highly dependent on favorable environmental conditions, coincident with the availability of a spawning population size above

some unknown critical level (Funk and Bracken, 1984). Thus, it seems likely that sablefish recruitment is driven primarily by ecosystem processes. We therefore hypothesize that a critical window for sablefish survival is bounded by egg/larval development in the offshore pelagic zone and "settlement" in nearshore YOY nursery areas—such that relative year-class strength is not substantially altered in the juvenile migration to the adult slope habitat, approximately two to four years later.

Early life stages of fish generally display weak swimming capabilities, and Lagrangian, spatially-explicit IBMs that track individuals in space and time have been established as a viable approach for exploring their transport (Bartsch et al., 1989; Hinckley et al., 1996; Werner et al., 2001, 1993). The IBMs used in previous "connectivity" studies have ranged from quite simple models with minimal behavior (DeCelles et al., 2015; Takeshige et al., 2015) to relatively complex ones including a full suite of bioenergetics (North et al., 2008; Parada et al., 2016), each with a degree of complexity reflecting the data available for a particular species and the research question of focus. The IBM model we present here for sablefish considers life stages from egg to newly-settled (YOY) juvenile, and can be considered of medium complexity.

With our model-based approach, we specifically address the hypothesis that *'Recruitment variability of sablefish is primarily influenced by variability in the proportion of young fish transported from offshore spawning areas to nearshore nursery areas due to interannual differences in the hydrography of the GOA.'* To address this hypothesis, we initially assess the likely strength and variability in the connection between potential sablefish spawning sites and nursery areas (connectivity), and then develop model-based indices of connectivity, along with indices of environmental variables that could impact young sablefish. Finally, linear models were constructed to determine the amount of variability in the stock assessment-based sablefish recruitment index that can be attributed to variability in the connectivity/environmental indices.

2. Method

2.1. Model Description

To explore sablefish connectivity throughout the GOA, a novel sablefish IBM was coupled to a pre-existing Eulerian hydrodynamic model of the region. The sablefish model was developed within the Dispersal Model for Early Life Stages (DisMELS) framework (Stockhausen et al., this issue). DisMELS is a NOAA product developed at the Alaska Fisheries Science Center. This model simulates early life history characteristics (e.g. spawning locations, larval behavior, and growth rates) of individual 'fish,' and determines their interaction with the environment and transport pathways based on predictions of environmental forcing from physical estimates of circulation (i.e. tides and currents) and scalar properties (i.e. temperature and salinity). The DisMELS model has previously been applied to study movements of early life stages of groundfish in the Bering Sea (Cooper et al., 2013) and market squid in the western Pacific (Kim et al., 2015). Further information on the DisMELS model can be found in Stockhausen et al. (this volume). The Regional Ocean Modeling System (ROMS) that provided the ocean circulation fields has been well documented elsewhere (Haidvogel et al., 2008; Moore et al., 2004; Shchepetkin and McWilliams, 2005), and so is not described here in further detail; however, its specific application to the GOA is outlined below. The IBM model was run for sixteen consecutive years, from 1996 to 2011, representing the longest time-period of output available from the computationally-expensive high-resolution ROMS ocean circulation model.

2.2. *Physical model*

The physical environmental forcing used to drive the sablefish IBM was derived from an implementation of ROMS for the GOA, with a horizontal resolution of approximately 3 km with ~500 × 500 grid points. Grid boundaries extend from the Shumagin Islands (162.74°W) in the western Gulf to Prince of Wales Island in the eastern Gulf (132.10°W), and from 46.66°N in the GOA basin up through Prince William Sound (64.19°N, Fig. 1). Vertical resolution of the GOA hydrographic model varies with bottom depth, as the model uses a stretched coordinate system with forty-two vertical layers. This approach ensures finer resolution in the upper water column to better resolve physical features important to biology. The minimum depth of the GOA model grid is 10 m, and the thickness of the upper layer varies from ~0.5 m over the continental shelf to ~5-10 m over the basin. Six-hourly Climate Forecast System Reanalysis (CFSR, Saha et al., 2014) atmospheric variables (wind velocities, air temperature, rainfall rate, absolute humidity, and downward shortwave and longwave radiation) were used to drive the model. The model receives boundary information from a coarser ~11-km resolution ROMS model that extends over the Northeast Pacific (Coyle et al., 2012). The application of ROMS to the GOA, as well as the model's skill in resolving common features in GOA circulation that can influence transport—such as currents, eddies, meanders, and hydrographic fronts—have been presented previously (Cheng et al., 2012; Coyle et al., 2013; Dobbins et al., 2009; Hermann et al., 2016, 2009; Hinckley et al., 2009), and so are not repeated here.

2.3. *IBM model*

The sablefish IBM is relatively simple, reflecting the limited knowledge we have for this species. The five life stages considered include fertilized eggs, yolk-sac larvae, feeding larvae, epi-pelagic juveniles, and 'settled' juveniles (Fig. 2). In the baseline model run, each life stage has different constant growth rates, depth preferences, vertical swimming speeds, minimum and maximum stage durations, and sizes that must be reached before transitioning to the next stage. The baseline value for each parameter used in the multi-year model simulations, and the assumed parameter distribution (minimum, maximum, and modal values) used in the sensitivity analysis, are shown in Table 1, along with references used to support parameter selection. While baseline growth rates are presently independent of the environment (e.g. they do not depend on temperature or food availability) and are set to ensure that all individuals would be able to reach an adequate size and transition to the next life stage in the designated amount of time, this is not necessarily true for the parameter combinations that are generated from the parameter sensitivity analysis (described below). The individuals in the model are presumed unable to exhibit complex horizontal movement behavior, but can control their vertical position in the water column. For each life stage, a "preferred" depth range and a mean vertical swimming (up/down) speed was defined. Individuals outside their preferred range undertook directed swimming (at a rate given by its mean vertical swimming speed) until they returned to their preferred depth range.

Daily averages for physical oceanographic fields from the GOA ROMS model, low-pass filtered to eliminate tidal aliasing, were used to drive the IBM simulations within the DISMELS framework. The IBM used a sub-daily integration time-step of twenty minutes to improve the accuracy of the Lagrangian tracking algorithm for movement, and to better resolve biological processes such as diel vertical migration. Transport of individuals was due to advection, as well

as vertical swimming or sinking. Within the DisMELS framework, locations of individuals on the ROMS grid were updated at each biological time step. Specifically, the three-dimensional currents from the ROMS model output were interpolated for each individual's location. Individual movement rates due to swimming or sinking were then converted to ROMS grid coordinates and added to the in-situ ROMS currents. A fourth-order predictor-corrector algorithm was then used to perform a Lagrangian integration, to determine the new location of the individual at the end of the time step. While there are a few ways to validate IBMs, including population genetics data, tagging, or frequent stage-specific targeted sampling throughout the model domain, none of these validation approaches is presently possible for our focal species, due to very limited data availability. However, the modeling results presented here could be incorporated into future sample design efforts to address this lack.

2.3.1. Egg stage

Individual 'sablefish' were initialized in the model at the egg stage. All eggs were assumed fertile, with the ability to develop to hatching stage. Eggs were released at five release times (r) between February 15th and June 15th (Feb. 20, Mar. 5, Mar. 20, Apr. 5, and June 5, Figure 3a), corresponding to the window of time that sablefish eggs have been observed in the GOA (Doyle and Mier, 2015). Although adult sablefish have been found from ~300 to 800 m depth (Hunter et al., 1989; Mason et al., 1983; Moser et al., 1994) on the outer shelf and upper slope in the North Pacific (Allen and Smith, 1988; McFarlane and Beamish, 1983), and young sablefish have been observed up to more than 150 km off of the Alaska coast (Moser et al., 1994; Wing and Kamikawa, 1995), no precise information on the spawning locations of sablefish in the GOA is currently available. As the level of spawning biomass is not closely related to sablefish recruitment (Shotwell et al., 2014), we simulated the release of egg particles over the entire continental shelf break, between the 500-m and 2000-m isobaths, with a vertical resolution of 50 m between 300 and 800-m depth (Fig. 1, Fig. 3b For each release, individuals were initialized in a 5 km × 5 km grid within each alongshore spawning area. On each of the five release days, 25,476 individuals were released, for a total of 127,380 individuals per annual simulation. The 5 × 5 km horizontal spacing was selected following a sensitivity experiment that found this resolution produces connectivity patterns analogous to those obtained from finer horizontal spacing (see results section), at a fraction of the computational cost—thus permitting a larger number of model experiments within the timeframe of the project.

To reflect current understanding of vertical positioning of eggs in the water column (Alderdice et al., 1988) following 'spawning' in the model, the eggs adjust their vertical position to maintain a depth between 213 and 360 m. Eggs are assumed to be 2 mm in diameter when first spawned with a growth rate of 0.28 mm/day. The minimum time required for eggs to develop and hatch into yolk-sac larvae is 11.25 days, and once a size of 5.35 mm is reached, eggs are assumed hatched. Eggs that fail to reach the minimum size required for transition to the next life stage within the allotted timeframe (twenty-seven days) are considered unsuccessful.

2.3.2. Yolk-sac larval stage

We assume that while yolk-sac larvae can regulate density to maintain vertical position in the water column after sinking to a depth of 500-1000 m, this stage does not actively swim—reflecting the fact that in the laboratory, newly hatched larvae did not exhibit spontaneous movement (Alderdice et al., 1988). Following a minimum of seven days at this stage, the larvae are assumed to have used up their yolk sac and will transition to feeding larvae, provided they

have reached a minimum size of 7 mm. The growth rate for this stage is 0.26 mm/day, and the maximum stage duration is set to twenty days.

2.3.3. Feeding larval stage

Larvae exhibit spontaneous movement at 455 h (~19 days) after fertilization (Alderdice et al., 1988), at which time they can actively swim toward the surface and join the neuston. In the model, we assume that following the transition to the feeding larval stage, individuals ascend rapidly in the water column until they reach the neuston, considered here to be the upper 1 m. Larvae actively maintain their position in the neuston through this life stage. Due to a lack of information relating sablefish growth to consumption, explicit feeding and resource-mediated growth by larvae is not represented in the IBM. Growth rate is assumed to be 0.48 mm/day. While there is no marked morphological change between the larval and juvenile stages (Kendall and Matarese, 1987), larvae are considered '*epi-pelagic juveniles'* once they have reached total length of 35 mm. Feeding larva that fail to reach this size within the specified timeframe are considered unsuccessful.

2.3.4. Epi-pelagic juvenile stage

Epi-pelagic juveniles continue to maintain their position in the neuston but grow at a much faster rate (1.8 mm/day) and have much greater swimming speed (0.1 m/sec) than the larval stages. Once individuals reach 150 mm they are considered *'Juveniles'* with the capacity to 'settle' in defined nursery areas.

2.3.5. Juvenile stage

Following the transition to the juvenile stage, individuals continue to inhabit the upper water column but undertake diel vertical migrations, moving higher in the water column at night (Courtney and Rutecki, 2011; Sogard and Olla, 1998). The growth rate of individuals at this stage decreases slightly, relative to the previous stage (1.47 mm day^{-1}), while swimming speed increases relative to previous stages (0.3 m s^{-1}). While juvenile sablefish do not "settle" in the common sense of the word (as they never fully transition from the pelagic environment to the benthic environment), acoustical tagging (Courtney and Rutecki, 2011) indicates they actively maintain their position over desirable habitats in shallow inshore bays. Throughout their study area in Southeast Alaska, Courtney and Rutecki (2011) found average water depth of age-0 juvenile sablefish to be 18.6 m. In St. John Baptist Bay, the average depth of tagged juvenile sablefish was 23.6 m. Because the minimum depth of the GOA model grid is 10 m, shallow inshore bays are not well resolved. We therefore used a deeper depth criterion (23.6 m) to specify when juveniles that find themselves over shallow water can transition to 'settled juveniles,' and when transport to a nursery area is deemed successful. The exact timing of migration to the bottom is unknown, but occurrence of individuals in bottom trawls suggests that at least some settlement occurs at the end of the first summer (Sogard and Olla, 1998). Here, we consider juveniles that fail to reach a suitable nursery habitat before December 31 (the end of the simulation) unsuccessful; this means that individuals spawned earlier in the year had longer to reach suitable settlement habitats than those spawned later in the year.

2.4. Analysis

To assess interannual variability in the transport of young sablefish from offshore

spawning to near-shore nursery areas, we used output from the sablefish model simulations to calculate probability of transport from a spawning area to a settlement area for each year. To compare interannual differences in connectivity, we looked at "total connectivity" (the probability of settlement integrated across all spawning areas) and connectivity to/from specific alongshore areas. We also used two different metrics—a structural similarity index (SSIM) and an empirical orthogonal function (EOF) analysis—to compare overall spatial patterns in connectivity. Annual indices from each of these connectivity analyses, along with annual indices of physical oceanographic variables and spring and summer primary production (simulated by the ROMS-NPZ model), were correlated with indices of annual (age-2) recruitment developed from the assessment model for the Alaska sablefish stock (Hanselman et al., 2014b). Simple linear models were constructed and analyzed to determine the percentage of sablefish recruitment variability that the models could explain. To help put some bounds on uncertainty in model estimates of annual connectivity, as well as determine which model parameters are the most sensitive, we conducted an in-depth sensitivity analysis of the sablefish IBM.

2.4.1. Connectivity Analysis

Information regarding the distribution of sablefish spawning stock is largely lacking. Therefore, we have made the simple assumption that sablefish spawning stock is uniformly distributed across all potential spawning areas. This assumption allows us to focus on evaluating the *relative* strength of connectivity from each large-scale (100s of km) potential spawning area to a number of similarly large-scale potential nursery areas. To assess the connectivity between simulated spawning and settlement sites throughout the GOA on a ~150-km horizontal scale, we divided the entire GOA into twelve approximately equal areas (Fig. 1), with the location of individuals at spawning assessed to determine which of the twelve alongshore zones each individual occupied. Similarly, the locations of individuals were assessed at the end of the model run to determine within which, if any, of the alongshore zones they settled.

For each model year (y), the strength of connectivity between the spawning and recruitment sites was calculated as the proportion of individuals released from a spawning area (s) that settled into a nursery area (n). Egg abundance data (Doyle and Mier, 2015) indicate an asymmetric triangular temporal distribution, with most eggs observed in mid-February and tapering in abundance through June. These egg abundance data were used to determine bi-weekly empirical proportions, which were then used to weight (w, Fig. 3a) the connectivity matrices ($C_{n,s}$) resulting from individual release time to derive an annual mean connectivity matrix ($\bar{C}_{n,s}$) for each year,

$$\bar{C}_{n,s}(\mathrm{y}) = \sum_{r=1}^{5} C_{n,s}(r) \cdot w_r \qquad (1)$$

Our annual connectivity matrices reflect the fraction of individuals released in each spawning area that were successfully "recruited" to each nursery area—independent of the size of the spawning stock in any spawning area. To explore the interannual variability in connectivity between spawning and nursery sites, we examined: 1) interannual variability in "total connectivity" (C_{TOT}), the sum of all probabilities in the connectivity matrix for each year; 2) interannual variability in connectivity from potential spawning areas through the GOA to nursery area 3 (C_{n3}), which includes St. John Baptist Bay, a known nursery area; and 3) the variability in connectivity from spawning area 1 in the easternmost Gulf, postulated to be the principal spawning grounds (Funk and Braken, 1984), to any nursery site (C_{s1}).

For each of the indices of connectivity (C_{TOT}, C_{n3}, C_{s1}), the annual standardized anomaly was computed for comparison with the recruitment index by:

$$x_s = \frac{x-\mu}{\sigma}, \tag{2}$$

where x represents the annual index (i.e. C_{TOT}), and μ and σ are the mean and standard deviation of x for 1996-2011, respectively.

To provide a measure of central tendency, the overall median connectivity for each cell in the matrix was computed from the annual connectivity matrices:

$$M_{n,s} = \text{median}\left(C_{n,s}(y)\right)_{y=1996}^{2011} \tag{3}$$

In addition, the overall temporal variability in connectivity was estimated using the temporal median absolute deviation (Leys et al., 2013) of the annual connectivity matrices:

$$\sigma MAD_{n,s} = \text{median}_{n,s}\left(abs\left(C_{n,s}(y) - M_{n,s}\right)\right) \cdot 1.4826 \tag{4}$$

To determine the relation between changes in connectivity for each pair of spawning and nursery areas, we employ multivariate empirical orthogonal eigenfunction (EOF) analysis, a proven method for analysis of data with complex spatial/temporal structures. EOF provides an efficient decomposition of a dataset into representative modes, by determining empirically the eigenfunctions that best describe the information (Kaihatu et al., 1998). The EOF method describes the data in terms of EOF eigen-modes, ordered by the percentage of the total variance explained by each of the modes, which are statistically uncorrelated with one another. Through EOF analysis, we derived spatial covariance across the series of annual mean connectivity matrices, for each of the sixteen years simulated. This allowed us to examine the covariance structure between spawning and nursery areas in the GOA in space and time. This analysis resulted in a set of spatial patterns ("modes") and the associated set of Principal Component (PC) time-series, the first and second of which we subsequently related to sablefish recruitment.

Mathematically, the EOF analysis operates as follows:

1) Calculate the "climatological" connectivity matrix from the series of annual mean connectivity matrices, summarizing the connectivity between each spawning (s)-nursery (n) area pair over P = 16 years:

$$\mathrm{C_{yr}(n,s)} = \sum_{\mathrm{y=1996}}^{2011} \mathrm{\bar{C}_{n,s}(y)}\ /\mathrm{P}$$

2) Subtract the climatological mean from each annual mean connectivity matrix, to obtain the annual anomalies for connectivity with zero mean:

$$\mathrm{C_{anom}(n,s,y)} = \mathrm{\bar{C}_{n,s}(y)} - \mathrm{C_{yr}(n,s)}$$

3) Permute the matrix to re-order elements in $\mathrm{C_{anom}}$ into array CM with dimensions y x (n*s).

4) F = detrend CM to remove the time mean.

5) Calculate the covariance matrix of the anomalies:

R = F * F'

6) Use the eig MATLAB function to compute Eigenvalues of the temporal covariance matrix R:

[E,L] = eig(R)

7) Obtain Principal Components by projecting eigenvectors on original data:

PC = E'*F

Cell-wise comparisons of the elements in a connectivity matrix may not provide a good measure of how any one connectivity matrix is different from another overall. As such, we used a structural similarity index (SSIM) from the field of image analysis (Wang and Bovik, 2009) to formalize 'visual inspection' of the entire connectivity matrix and compare the overall 'quality' of an individual year's connectivity matrix to the median connectivity matrix. SSIM is a compound measure of the similarities of three elements—luminance (l), contrast (c) and structures (s)—between local image patches *x* and *y*. To apply SSIM to the connectivity matrix, we first converted the probabilities that comprise individual connectivity matrices to a measure of image brightness (greyscale) by scaling between 0 (black) to 255 (white). The SSIM index is computed locally (S(*x,y*)), within a sliding window that moves pixel-by-pixel across the images, comparing equivalent patches (x and y) in the two images (Equation 5):

$$S(x,y) = l(x,y) \cdot c(X,Y) \cdot s(x,y) = \left(\frac{2\mu_x\mu_y+\mathrm{c}_1}{\mu_x^2+\mu_y^2+\mathrm{c}_1}\right) \cdot \left(\frac{2\sigma_x\sigma_y+\mathrm{c}_2}{\sigma_x^2+\sigma_y^2+\mathrm{c}_2}\right) \cdot \left(\frac{\sigma_{xy}+\mathrm{c}_3}{\sigma_x\sigma_y+\mathrm{c}_3}\right) \qquad (5)$$

and

μ_x and μ_y are the local sample means of **x** and **y**,
σ_x and σ_y are the local sample standard deviations of **x** and **y**,
σ_{xy} is the sample cross correlation of **x** and **y** after removing their means, and
$\mathrm{c}_1 = (0.01 \cdot L)^2$, $\mathrm{c}_2 = (0.03 \cdot L)^2$, and $\mathrm{c}_3 = \mathrm{c}_2/2$ are small positive constants that stabilize each term and ensure that sample means, variances, or correlations close to zero do not lead to numerical instability, and $L = 255$—the dynamic range of the image.

The local patch window was determined using a rotationally symmetric 2-d Gaussian low-pass filter with 3 × 3 'pixels' and a standard deviation of 0.5. The relatively small filter window was chosen because it enabled two images (connectivity matrices) that were similar, i.e. the connectivity between spawning and nursery areas had been shifted only slightly east or west, to be quantified as such. A simple direct comparison of each cell in the connectivity matrix (image pixel) without filtering would underestimate the similarities in connectivity. The SSIM score for the entire image is computed by averaging the images' local SSIM values, with a value from -1, indicating the images are perfectly negatively correlated, to 1, indicating that the images are identical. Figure 4 illustrates how the SSIM index I interprets differences between connectivity matrices, by comparing a reference matrix consisting of only numbers along one

diagonal (Fig. 4a) to several perturbations of this reference matrix.

2.4.2. Environmental indices

Annual environmental indices were derived from the ~3-km ROMS hydrography model (salinity and temperature) used to drive the IBM, and from the lower trophic level Nutrient-Phytoplankton-Zooplankton model (primary production). Model estimates of primary production in the GOA have been well validated (Coyle et al., 2012, 2013), and we use this variable as a proxy for the secondary production (by zooplankton) that young sablefish would consume. Because nursery grounds from southeast Alaska to British Columbia are known to be some of the most important for young sablefish (Rutecki and Varosi, 1997; Sasaki, 1985), we consider indices for the eastern (east of 147°W) shelf region, extending from the shore to the 200-m isobath, and the eastern offshore region, extending from the 200-m isobaths to 200 km off the shelf break. The east/west division of the Gulf was based on the finding by Mueter *et at*. (2016) that a significant break point in multiple bio-physical variables—a natural dividing line between the eastern and western GOA—is centered near 147˚W -148ºW. The indices in the offshore region were developed for spring (April and May), as this is the time period when young sablefish are most likely to be in this region. Indices for the on-shelf region were developed for the summer (June-August), as the importance of this region is thought to increase as sablefish mature and move on to the shelf. Salinity and temperature indices were for the upper 10 m, while primary production was integrated over the upper 30 m of the water column. For 1997-2011, a cross-shelf velocity index was developed from a coarser (~11 km) version of the ROMS model previously run over the Northeast Pacific (Danielson et al., 2011). Modelled velocities were interpolated to the locations of the 500-m isobaths along the shelf break, and rotated to determine cross-shelf flow (i.e. flow perpendicular in direction to the shelf edge). We considered annual average cross-shelf velocity anomalies binned over the western (150°-155°W), west-central (145°-150°W), and east-central (140°-145°W) Gulf separately. As with the indices for connectivity, environmental indices were standardized following the formulation in Equation 2, and used to examine the relationship between the environment and sablefish recruitment, as described below.

In a subsequent exploratory analysis, the relationship between sablefish recruitment and wind direction over the Eastern Gulf of Alaska (~55.1-62°N, 130-145°W), as predicted by the Climate Forecast System Reanalysis model (CFSR, Saha et al., 2014), was examined. This was the same atmospheric model product used to drive the 3-km ROMS circulation model that drives the IBM. For each time period considered (January-February, February-March, March-April, April-May, May-July), wind indices were developed by computing the percentage of time-steps with average southerly, easterly, and south-easterly wind over the eastern and western Gulf of Alaska.

2.4.3. Lower trophic level model indices

The sablefish IBM in its present configuration does not include food-dependent growth rates or movement. To explore the potential impact that food availability could have on the early life stages of sablefish, we analyzed primary production estimates simulated by an Eulerian, lower trophic level Nutrient-Phytoplankton-Zooplankton (NPZ) model. The NPZ model was coupled to the same ROMS physical model used to drive the IBM experiments, and was run for the same 1996-2011 time period as IBM simulations. The NPZ model consisted of eleven components: nitrate, ammonium, detritus, iron, small phytoplankton and large phytoplankton,

small and large microzooplankton, *Neocalanus* copepods, 'other' copepods, and euphausiids. Here we used the spring and summer integrated primary production over the upper 30 m in the eastern inshore and offshore regions to complete our set of annual environmental metrics for comparison to sablefish recruitment indices. A full description of the model and its skill in predicting primary production can be found in Coyle et al. (2013, 2012).

2.4.4. Recruitment

The Stock Assessment and Fishery Evaluation (SAFE) report produced for the North Pacific Fishery Management Council includes annual estimates for sablefish recruitment in Alaska (the abundance of age-2 sablefish entering the Alaska-wide stock), for the years 1933-2013 (Hanselman et al., 2014b, Table 3.14). Variability in sablefish recruitment was estimated using an age-structured assessment model as log-scale deviations from a long-term mean, rather than using a stock-recruitment relationship (Hanselman et al., 2014b). This assessment model incorporates information about female maturity-at-age, length and weight at age, relative abundance, age compositions, and natural mortality data. Annual recruitment estimates (R) can vary by orders of magnitude, so following the assessment model, we analyzed the recruitment time-series on the log scale, which we standardized (R_s) for comparison to the standardized connectivity and environmental indices using:

$$R_s = \frac{\log\frac{R}{\bar{R}} - \text{mean}(\log\frac{R}{\bar{R}})}{\text{std}(\log\frac{R}{\bar{R}})} \quad . \tag{6}$$

The standardized recruitment index for sablefish from 1959 to 2014 is presented in Fig. 5a, with the shorter focal period for this study presented in Fig. 5b. The stock assessment model estimates sablefish recruitment strength as the number of fish at age-2 (Hanselman et al., 2014b). For correlating recruitment indices with modelled connectivity and environmental indices, the shorter time series was shifted back two years, such that the recruitment index corresponds to the year in which individuals were spawned.

Pearson's r correlation coefficient was used to determine which of the standardized indices had a stronger relationship to recruitment, and the direction of that relationship. Simple linear regression models were constructed using indices with the highest correlations to recruitment as predictors, and with recruitment as the response. Only the main effects from each predictor were considered. The F-statistic was examined to test the null hypothesis that all regression coefficients were not statistically different from zero, and the coefficient of determination (R^2) was computed to assess the strength of the relationship between the predictor(s) and the recruitment index. For models with more than one predictor, we used adjusted R-squared to compensate for the loss of degrees of freedom.

2.5. Sensitivity Analyses

2.5.1. Horizontal resolution

Prior to running the multi-year model experiment, a sensitivity analysis was performed to explore the sensitivity of model results to the horizontal resolution of the release locations for individuals. In this experiment, individuals were released in spawning zone 2 (southeast GOA), and the probability of settlement within each of the twelve alongshore nurseries was determined. All individuals were released on February 20, 2003. Vertical spacing was consistent at 50-m

depth levels between 300 and 800 m throughout the water column, while the horizontal resolutions explored included 0.5 km, 1 km, 5 km, 10 km, 15 km, 20 km and 25 km.

2.5.2. Parameter uncertainty

Understanding the impact from parameter uncertainty on model estimates of connectivity will permit a more accurate interpretation of model estimates of interannual variability due to changes in the physical environment alone. Despite its commercial importance, the sablefish is a relatively understudied species, and many parameters and mechanisms pertaining to its behavior are not well known. As such, this first iteration of the sablefish model is relatively simple and lacks the complexity of a full bio-energetics model. In addition to assessing model predictions of interannual variability in GOA sablefish connectivity, we assessed the sensitivity of the model to parameter choice, and the relative impact of each parameter on model uncertainty. Most commonly, sensitivity of an IBM centers around model behavior under certain 'scenarios'; that is, a few fixed parameter values (see Garavelli et al., 2014). Megrey and Hinckley (2001) used a more comprehensive Monte Carlo approach to assess the influence of turbulence on feeding, growth, and mortality of larval walleye pollock. Here we use this more comprehensive approach to explore model sensitivity by varying multiple model parameters simultaneously.

The parameter sensitivity experiment was conducted using physical forcing and egg distribution from the 2002 baseline experiment—i.e. eggs were initialized at 5 × 5-km resolution between the 500 and 2000-m isobaths, at the same 50-m depth levels between 300 and 800 m, as used in the baseline experiment. Egg release was February 20, corresponding to the time of peak egg abundance in the western GOA (Doyle and Mier, 2015). The parameter sensitivity analysis used a Monte Carlo style exploration of model predictions, varied by 37 model parameters. A stratified Latin hypercube sampling procedure was used to generate 500 input parameter sets by drawing parameter values from their specified triangular probability distributions, assuming independence between parameters. Unless indicated otherwise (Table 1), the baseline values used in the multi-year runs were used as the mode for distribution, and upper and lower limits for parameter distributions were based on ranges presented in the literature, or where this information was not available, ±10 % of our baseline value.

To rank the contribution from each of the parameters to the model output uncertainty, we used Least Squares Linearization, a multiple regression between the parameters' deviation from the mean and the model output (Gibson and Spitz, 2011; Verbeeck et al., 2006). The uncertainties for each parameter were used as independent variables for the regression equation, with model outputs as dependent variables. We explored the sensitivity of the model using four output variables as different measures of spawning-nursery connectivity: 1) the total connectivity between spawning and nursery areas (C_{TOT}); 2) the proportion recruited to nursery areas in the alongshore zone 3 (C_{n3}), the location of St. John Baptist Bay, a known nursery area; 3) the proportion recruited from spawning areas in alongshore zones 7 and 8 (C_{s78}), which encompass the majority of the locations in which Doyle and Mier (2015) observed eggs; and 4) the structural similarity index, comparing each of the 500 connectivity matrices to the median connectivity matrix ($SSIM_{500}$). For each of these four output variables, parameters were ranked according to the magnitude of their sensitivity parameter (S_{v_i}),

$$S_{v_i} = \frac{w_i^2 \cdot \sigma_{\delta v_i}^2}{\sigma_{\delta y}^2} \cdot 100\% \quad , \tag{7}$$

where regression coefficients (w_i) were estimated by minimizing the sum of square errors and used to calculate the overall variance ($\sigma^2_{\delta_y}$) in model output for each parameter. Analysis of variance was performed to determine the percentage of variability in model output that could be attributed to the top ranked parameters.

2.5.3. Depth of settlement

In-depth parameter sensitivity analysis indicated that depth of settlement was a critical factor to model predictions regarding connectivity between spawning and nursery areas. As such, we performed additional sensitivity analysis in which baseline parameter values were used, but settlement depth was set to 15 m, 20 m, 50 m and 100 m. In this model experiment, eggs were released throughout the spawning zone at the same depth levels and on the same date (February 20, 2003) as the main sensitivity experiment. For each model run, the strength of connectivity between the spawning and recruitment sites was calculated as the proportion of individuals released from a spawning area (s) that settled into a nursery area (n), and connectivity matrices ($C_{n,s}$) were constructed and compared. Each of the four resultant connectivity matrices were scaled by their respective maximum probabilities, to better enable the connectivity patterns between spawning and nursery areas to be compared. In the absence of scaling, the similarities in patterns are overshadowed by the simple fact that more individuals could settle in all alongshore zones as the settlement depth criteria increased because individuals are less reliant on transport to shallow coastal areas before settlement could occur.

3. Results

3.1. Connectivity from spawning areas to recruitment sites

Over the sixteen-year period examined, maximum connectivity between an individual spawning area and an individual nursery area was 0.17; this maximum connection was from spawning area 3 to nursery area 5 in 1996. The maximum probability for an individual released in a spawning area to settle in any of the twelve nursery areas was 0.38. This maximum probability was also for individuals released in spawning area 3 in 1996. On average, 56.8 % (SD = 8.6 %) of all individuals released each year were transported out of the model domain through the southwestern model boundary (West of the Shumagin Islands, west of 159°W, north of 51°N). An average of only 5.5 % (SD = 3.1 %) of all individuals released each year were transported out of the model domain through the southeastern model boundary (east of 135°W and south of 55°N, just north of Haida Gwaii).

Individuals successfully settling in any nursery area within the model domain were significantly more likely to have been spawned in the eastern Gulf (alongshore spawning regions 1-5) than the western Gulf (7-12, Fig. 6). Spawning areas 2 and 3 were equally likely the most successful source locations (median probability ~0.25). It is likely that spawning area 4 would produce less successful settlers (median probability ~0.2) than these primary regions, while individuals released either in spawning area 5 or 1 had a significantly smaller chance (probability 0.15 and 0.1, respectively) of successful settlement in a nursery area. Individuals spawned in the western Gulf (alongshore areas 7-12) were likely to have only a 0~0.05 % chance of successful transport and settlement into a nursery area in the GOA.

The annual median pattern of connectivity (Fig. 7a) in the GOA suggests a generally westwards transport of individuals from spawning sites to nursery grounds. Although interannual

variability in median connectivity (Fig. 7b) was sometimes of a similar order of magnitude to the median suggesting that connection (probability of successful transport and settlement) between some regions varied quite strongly, interannually. Some clear patterns emerged, with some spawning/nursery areas much more strongly connected than others. The strongest connectivity was from spawning areas in the eastern Gulf to nursery areas in the central Gulf. Spawning area 3 (Cross Sound) and nursery areas 5 (Icy Bay region) and 6 (PWS region) were relatively strongly connected (Fraction Settled ~0.1), as were spawning area 2 (Sitka region) and nursery area 5. The connection between spawning area 2 and nursery area 4 (Yakutat region) was also relatively strong, as was the connection from spawning area 5 to nursery area 9 (southern Kodiak region) compared to other pairwise connections. As indicated in Fig. 6, by and large, spawning areas in the western Gulf (areas 7-12) were only weakly connected (if at all) to any nursery area. The connection between spawning area 2 and nursery area 5 was the most variable (Fig. 7b). The probability of an individual making it to settlement stage but unable to settle due to offshore transport to the basin (Fig. 7c) was highest for individuals spawned in areas 7-9 (Kenai and Kodiak regions). Individuals spawned in areas 1-4 had the highest probability of settlement—thus transport to the basin from these areas was low. Transport to the basin from spawning areas 11 and 12 was also low, but individuals released in these areas were more likely to be transported out of the domain than onshore to a nursery area.

Annual deviations from median connectivity between spawning and nursery areas show that the change in strength of the pairwise connections was generally not homogenous throughout the model domain (Fig. 8); in any one year, some spawning and nursery areas had a stronger than median connection, while others had a weaker than median connection. Deviation from the median probability of settling in the easternmost (1 and 2) and westernmost (11 and 12) nursery areas was low for all years, as was the probability of settling in a nursery area when spawned west of area 7 (Kenai). In contrast to the interannual deviations in connectivity seen for nursery areas 6 and 8, in most years the probability of individuals spawned throughout the model domain settling in area 7 was close to the median, which was relatively low. The spatial pattern of positive and negative deviations in connection strength varied year-to-year, but similar spatial patterns emerged in some years. For example, 1996, 1997, and 2002 were years with generally positive deviations from median connectivity over much of the connectivity matrix, suggesting that in these years, the successful transport and settlement of individuals from spawning sites to nursery areas was relatively high overall. In 1996 and 2002, there was a relatively large increase in the strength of the connection, relative to the median, from spawning areas 3 and 4 to nursery area 5, but a small decrease in the connection from spawning area 1 to nursery areas 5 and 6. In 1998, retention in the same region (i.e. simple onshore movement from spawning to nursery area within the same alongshore zone) was increased relative to the median, as was the strength of the connection to the region immediately downstream (west); however, spawning areas 1-5 were less strongly connected to nursery areas farther west (three regions away). A similar shift in connectivity was also observed in 2002. Years 1999 and 2008 also shared similar patterns in the strength of connectivity between spawning and nursery sites, with much stronger than median connectivity from spawning areas 1-3 in the east to nursery areas 4 and 5 farther west, as well as some below-median connectivity from spawning areas 4-6 to nursery areas farther west. As in 1999 and 2008, in 2000 the positive deviation between spawning areas 1-2 and nursery areas 4-5 was relatively large, but there was above median connectivity between spawning areas 1-5 and most of the nursery areas farther west. In 2004 and 2009, spawning areas 1-3 had a decreased connection to nursery areas 5-6, but there was an increased connection between most other

spawning-nursery area pairs. A similar pattern was observed in 2005, but then it was nursery areas 4-5 that showed a decrease in the probability of settlement. Year 2003 had the smallest deviations, either positive or negative, indicating the connectivity between the spawning and nursery sites for this year was most similar to median connectivity (Fig. 7a).

Total probability of connection summed over the connectivity matrices (Fig. 10a) did not correlate strongly with connectivity to sites containing known nursery areas (i.e. St. John Baptist Bay) or with connectivity from the easternmost spawning site. Total probability of settlement for individuals released from any spawning area (C_{TOT}) indicates that prior to 2005, C_{TOT} was more variable, oscillating above and below the median year-to-year (Fig. 10a). After 2005, year-to-year changes in C_{TOT} were smoother—initially increasing (2005-2007), and then remaining steady for three years (2007-2009), before progressively decreasing in 2010 and 2011. Years 1997 and 2002 showed the strongest overall connectivity between spawning and nursery sites, while 2005 and 2011 were years of notably low connectivity. The probability of any individuals settling in nursery area 3 (C_{n3}, Figure 10b, black line) was only weakly correlated ($r = 0.35$, $p = 0.19$) to C_{TOT}. In this index, 2005 was also a year of below-median connectivity, though 1999, rather than 1997, showed strongest connectivity. The correlation between C_{s1} (Fig. 10b, grey line) and C_{TOT} was even weaker ($r = 0.19, 0.48$), although both indices highlighted 1998 as a year with weaker than median connectivity. The probability of an individual released in spawning area 1 settling in any nursery area was relatively high for both 2006 and 2008, although overall connectivity was at a median level in these years.

The dominant patterns in relative connectivity between spawning and nursery area pairs throughout the 16-year period examined are underscored in the EOF analysis (Fig. 9). The first principal component of the EOF analysis explained ~38 % of the total variance and crosses the zero line, indicating there are spawning/nursery area pairs whose connectivity rise and fall in opposition throughout the time series, rather than together. This primary mode indicates that when alongshore retention (i.e. settlement in a nursery area in the same alongshore zone as the spawning area) is above average, the probability of individuals released in the western spawning zones (8-10) successfully settling in any nursery area is also above average. Conversely, during these times the probability of individuals released in eastern alongshore zones 1-3 successfully settling in a nursery zone was below average. In particular, the probability of settling in nursery areas 4-6 is far below average. The second principal component of the EOF analysis explained an additional 21 % of the total variance, and also crosses the zero line. This second mode indicates that in the eastern Gulf, when the probability of settlement in a nursery area immediately adjacent (downstream, to the west) of the spawning area increases, the probability of settlement in the next closest area (to the west) does also, meanwhile the probability of these individuals settling in a nursery area in the central and western Gulf is reduced. During this mode of variability, the probability of individuals released in the western Gulf settling in spawning zones 10 and 12 was above average. The first principal component (PC1) of the EOF analysis (Fig. 10d, black line) was strongly negatively correlated to C_{TOT} before 2002 ($r = -0.83$, $p= 0.04$), but the relationship did not hold in subsequent years ($r = -0.15$, $p=0.7$). Over this latter period (2003-2011), PC1 (Fig. 10d, black line) was strongly negatively correlated to C_{s1} ($r=-0.90$, $p<0.01$, Fig. 9c). The 2nd principal component (PC2, Fig. 10d, grey line) was positively correlated with C_{TOT} ($r = 0.58$, $p=0.02$) and to C_{n3} ($r = 0.61$, $p=0.01$), and highlighted 1996, 2005, and 2006 as years that were notably different from the median pattern of connectivity. Principal component 1 (PC1) and 2 (PC2) were not significantly correlated with recruitment (Fig. 10di, $r = -0.21$ and $r = -0.03$ respectively and $p >0.05$).

The SSIM index (Fig. 10c) also highlighted 1998 as a year with a pattern of connectivity between spawning sites and nursery areas very different from the median connectivity matrix. SSIM was reasonably well correlated with C_{TOT} for the 1996-2010 period (r = 0.56), but this relationship is weakened if 2011 is included, as 2011 had a strongly above-average SSIM index (i.e. close to median connectivity when considering the overall pattern of connectivity), but low overall connectivity C_{TOT}. As reflected by a relatively high SSIM value, 2003 was also a year in which the connectivity in the Gulf had an overall pattern close to the median connectivity pattern.

3.2. Correlations between settlement potential, environmental indices and recruitment

Considering how each of the indices that quantify interannual variability in settlement potential correlates with recruitment (Fig. 10 ai-ei), we found that recruitment was only weakly negatively correlated with the SSIM index and with indices derived from the individual components that compose the SSIM index (Table 2). With an r of 0.45 (p=0.08), the simple index of total connectivity between spawning and nursery areas was much more strongly correlated to recruitment than the SSIM index, although even this relationship was significant only at the 10% level. Correlations between recruitment and the fraction of individuals released in spawning area 1 as well as the fraction of individuals from all spawning sites that recruited to nursery areas 3 were also positive, but not as strongly. C_{TOT} was not correlated to the west-central or east-central Gulf cross-shelf flow (r = 0.27 and r = -0.12, respectively), or to the southwesterly wind index (r = 0.15). C_{TOT} was correlated to the western Gulf cross-shelf flow r=0.5258, p= 0.04.

Indices of salinity and temperature (Fig. 10d) in the eastern inner and outer domains during spring and summer did not correlate strongly with recruitment. The correlation between recruitment index and spring salinity in the eastern offshore region was weak but positive (i.e. increased salinity was associated with increased recruitment). Conversely, correlation between recruitment and spring temperature was weakly negative (increased temperature was associated with decreased recruitment). The extremely small negative correlations between the recruitment index and summer salinity or temperature anomalies in the eastern inshore region suggest there is no relationship between these variables. Both spring offshore primary production and summer onshore primary production (Fig. 10e) were positively correlated to recruitment and the strength of the correlation was comparable to that seen with Total Connectivity. Cross-shelf flow over the west-central Gulf was positively correlated with recruitment (r = 0.56, p = 0.03), though cross-shelf flow in the western and east-central Gulf was not correlated (r = 0.39 and -0.09 respectively).

An ANOVA linear model, constructed using *Total Connectivity* (C_{TOT}) and the environmental indices with the highest correlations to recruitment as predictors, and recruitment as the response, indicated that each of the predictors alone were significant at the 0.1 level but not at the 0.05 significance level (Table 3). Based on the R-squared values, these variables could account for 19-22 % of the variability in sablefish recruitment. Combining *Total Connectivity* with *Offshore Spring Primary Production* (PP_{SprR5}) resulted in a linear model that was significant at the 0.05 level and explained 28 % of recruitment variability. C_{TOT} and *On-shelf Summer Primary Production* (PP_{SumR4}) explained 26 % variability, but this model was only significant at a 0.1 level. Adding *Annual cross-shelf flow* to C_{TOT} increased the linear models explanatory power to 44 % ($p < 0.05$). Additionally, including PP_{SumR4} only increased the explanatory power by 1 %. Using PP_{SprR5} and PP_{SumR4} together in a linear model could account

for 42 % of the recruitment variability ($p = 0.01$), and adding in C_{TOT} increased the model's explanatory power to 51 % ($p = 0.01$). Our best model ($R^2 = 0.59$, $p < 0.05$) included C_{TOT}, annual cross-shelf flow, and both spring and summer production.

3.3. Sensitivity analyses

3.3.1. Horizontal resolution

A sensitivity analysis of the model output to horizontal resolution of egg initialization found that the probability of individuals settling in any nursery area was broadly similar, regardless of their initial spacing (Fig. 3c). When individual eggs were released 25 km apart, only 77 individual eggs were released per simulation in spawning area 2. Even with this small number of individuals, the probability of connectivity to each nursery area indicated that individuals were most likely to be transported to nursery area 5 or 6. This is in-line with connectivity patterns seen when the density of individuals spawned is greater. As the spawning resolution in area 2 was increased from the initial spacing of 25 km to 1 km, the pattern in probability of transport to each of the twelve nursery areas became more similar to that obtained with the finest resolution (0.5 km). An initial spacing of 5 × 5 km produced a pattern of connectivity between spawning area two and the twelve nursery area very similar to that obtained with the highest spatial resolution tested. The 5 × 5 km horizontal resolution had the advantage of being much more computationally efficient relative to a higher resolution initialization. For example, 1882 individuals were initiated in spawning area 2 per simulation using a 5 × 5 km spacing, compared to 47,579 individuals when using a 1 × 1 km spacing, and 190,164 individuals when using 0.5 × 0.5 km spacing. As such, we determined that 5 × 5 km spacing was optimal because it was capable of producing results very similar to a release with ten times greater resolution, while being manageable enough to allow completion of all model experiments within the time frame of the project, with the resources available to us. Following these findings, the intermediate 5 × 5 km resolution was used to initiate individuals in all remaining model experiments.

3.3.2. Parameter uncertainty

Overall, the spatial pattern for the median connectivity matrix arising from the parameter sensitivity analysis of the model (Fig. 11a) looked similar to the median connectivity matrix for the sixteen-year run (Fig. 7a). The pattern of prevailing westward connection between spawning and nursery areas was preserved, with low retention of individuals within any alongshore area and virtually no connectivity to nursery areas east of the spawning area. As was the case for the climatological median connectivity, the probability of transport from spawning to nursery areas was highest from areas 2-4 in the eastern Gulf to areas 5-6 in the central Gulf, and there was a low probability of individuals settling in any nursery area if released in the western Gulf (spawning areas 6-12). The median absolute deviation (Fig. 11b) associated with median connectivity from the sensitivity analysis also had a similar spatial pattern and magnitude relative to deviations associated with the annual median matrix (Fig. 7b). Despite the similarities in relative strength of connections between spawning and nursery areas in the annual median connectivity matrix and the median connectivity of all the sensitivity simulations, the median of the sensitivity matrix had a stronger (~1.5 times) probability of connection between most spawning and nursery pairs. Notably, the probability of successful settlement for eggs released from spawning site 4 into neighboring alongshore nursery area 5 was approximately five times

greater than seen in the climatology. The westernmost nursery area in the model domain (area 12) also saw a large increase in the number of probable settlers from spawning areas 5-9.

The total connectivity between spawning and nursery areas (C_{TOT}), the proportion recruited to nursery areas in alongshore zone 3 (C_{n3}), and the proportion recruited from spawning areas in alongshore zone 7 and 8 (C_{s78}) were all most sensitive to h_s, the settlement depth assigned to the juvenile stage (Table 4). The structural similarity index ($SSIM_{500}$) was most sensitive to the minimum size that must be reached before epi-pelagic juveniles can transition to the Juvenile life stage (ts_P). The 2nd-5th ranked parameters for the four diagnostic variables showed more variability, although several parameters were highly ranked for multiple variables. For example, the minimum epi-pelagic transition size was also highly ranked (2nd) for C_{n3}, and the swim speed of the feeding larvae (v_F) was ranked 2nd, 3rd, and 5th for C_{s78}, $C_{TOT,}$ and C_{n3}, respectively. Egg growth rate (g_E) was ranked 3rd and 4th for C_{s78} and C_{n3}, respectively, and the minimum night-time depth for the juvenile stage (zn_{minJ}) ranked 3rd and 5th in sensitivity for $SSIM_{500}$ and C_{TOT} variable, respectively. All other parameters that ranked within the top five for the four diagnostic variables were either related to the depth of the life stage in the water column, or to the size at which a stage transitioned to the next life stage.

The top five (Top_5) ranked parameters for each of the diagnostic variables accounted for between 58 and 78 % of the variability in C_{s78}, $C_{TOT,}$ and C_{n3}, respectively (Table 5). Variability in the five top ranking parameters for $SSIM_{500}$ could account for only 4 % of the variability in this variable. Considering the variability in the next five parameters also (i.e. Top_{10}), the variability explained in any of the four output variables increased by only 1-2 %. Removing h_s, the settlement depth assigned to the juvenile stage, from the analysis revealed how sensitive these model results are to this parameter, as the explanatory power of the remaining four (Top_4*) parameters was reduced to 1-24 %, depending on the output variables considered. The poor explanatory power of any of the parameters for explaining the variability in $SSIM_{500}$ can be accounted for by the fact that a slight right or left or up or down shift in the overall connectivity pattern between spawning and nursery areas would be interpreted by the index in essentially the same way, i.e. the response from SSIM to parameter change was non-linear.

3.3.3. Depth of settlement

Although the settlement depth parameter (h_s) was the most critical parameter for determining model estimates of connectivity between spawning and nursery areas, a sensitivity analysis focused on this parameter indicates our connectivity results are relatively robust to a broad range of its values (Fig. 12). For example, regardless of settlement depth criteria, there is a strong likelihood that individuals will have the greatest connectivity to a nursery area located to the west of their spawning location. As in the main experiment, some of the strongest connectivity was between spawning areas in the east (alongshore zones 2-4) and nursery area 5 and 6 in the central Gulf. Likewise, regardless of the settlement depth criterion, individuals spawned in the western Gulf were unlikely to settle in the GOA. The moderate connection to nursery area 9 (southern Kodiak region) that we noted in the main experiment was more likely with a shallower settlement depth, and less likely as the settlement depth criterion increased.

4. Discussion

As is true of all models, there are several assumptions we had to make, and which should be taken into consideration when interpreting our sablefish IBM results. Our model sensitivity analysis helped address implications of uncertainty around model parameters, and has suggested where additional studies (for improving error bounds around influential parameters) could improve model accuracy. Although the 3-km ROMS model used to drive the sablefish IBM is considered a relatively fine resolution for a basin-scale model covering a region as broad as the GOA, it undoubtedly misses some finer spatial and temporal dynamics, which could be important in transporting sablefish to nursery areas. Nevertheless, this model has previously been shown capable of resolving oceanographic features (e.g. eddies, ACC, Alaska stream) important to transport in the GOA (Cheng et al., 2012; Coyle et al., 2013; Dobbins et al., 2009; Hermann et al., 2016, 2009; Hinckley et al., 2009), and we believe our novel sablefish IBM can provide understanding about the strength of connections between potential spawning and nursery sites in the GOA. Specific implications of model shortcomings and assumptions are addressed as we discuss insights gained from the study.

4.1. Model sensitivity

The sensitivity of a particle tracking model for the assessment of larval transport has been largely overlooked. Simmons et al. (2013) investigated the sensitivity of 'larval' transport predictions to the number of particles released, particle release depth, and particle tracking time, using a biophysical model of the Southern California Bight although in their model, 'larvae' were passive particles absent of any biological characteristics. They found that the model's 'larval' transport predictions were sensitive to changes in the number of particles released, particle release depth, and particle tracking time. In our study, we released individuals (as eggs) at multiple depths through our model domain, and on multiple days throughout the known spawning period, such that we would encapsulate some of the variability associated with spawning. Our spawning resolution sensitivity analysis indicated that for our model study, based in the Gulf of Alaska, a horizontal resolution of 5 km for individual egg release produced similar results to a finer resolution (1 km) release, at a fraction of the computational cost. Decisions regarding the appropriate number of particles, their spacing, and release timing should be study-specific, as this depends on the physical dynamics of the region and the biological traits of the organisms in question.

Our parameter sensitivity study indicates that settlement depth was the most influential parameter for the model outputs we examined, which were various measures of potential connectivity between spawning and nursery sites in the GOA. The minimum size that must be reached before epi-pelagic juveniles can transition to the juvenile life stage, egg growth rates, feeding larvae swimming speed, and the depth preference of the juvenile stage were also influential parameters in determining connectivity. These parameters influence model output by determining the length of time (and thus distance) that individuals will be advected, and the current profile to which they are exposed. The only other in-depth sensitivity analysis of a marine IBM of which we are aware is by Megrey and Hinckley (2001), on an IBM for walleye pollock. They used a stratified Latin hypercube sampling procedure, equivalent to the approach implemented in the present study, to determine the relative importance of various feeding-related factors on larval growth and mortality. Reactive distance, minimum pursuit time, and weight-length conversion parameters were found as the most important input parameters. In that study, individual larvae particles were only tracked for eighty days, and the impact of parameter

variability on settlement was not considered. Because of the notably different model structure and goals of this study, it is not really meaningful to compare the parameters ranked as sensitive in each case. The differences do, however, highlight the need for sensitivity analysis to be study-specific, as the parameters that rank as most important in determining model output will likely vary widely, depending on the diagnostic under consideration.

4.2. The east to west connection

Our sablefish modelling study indicates that as young sablefish in the GOA progress from the egg stage to settled juvenile stage, there is a dominant pattern of westward transport, as successfully settling individuals move from spawning areas on the continental slope and towards inshore nursery areas. This is in line with the paradigm for sablefish movement—that small fish move westwards from their nursery areas, while adult fish move eastwards back to their spawning grounds (Echave et al., 2013; Heifetz and Fujioka, 1991). Recent tagging studies suggest that this overall movement pattern is probably more ambiguous than previously thought, as movement probabilities varied interannually and are negatively correlated with female spawning biomass (Hanselman et al., 2014a). The east to west connection between alongshore spawning and nursery areas in the Gulf reflects the dominant circulation patterns in the region, which include the Alaska Current that flows north-west along the coast of British Columbia and the Alaska Panhandle (Schumacher and Reed, 1987) and continues into the Alaska Stream, a fast westward flowing boundary current over the shelf break (Reed, 1984). Further inshore, the buoyancy-driven Alaska Coastal Current also flows in an anti-clockwise direction within about 50 km of the coast (Royer, 1998; Stabeno et al., 2004).

4.3. On-shelf advection

The GOA has multiple hydrographic fronts that can hinder on-shelf transport (Belkin et al., 2003, 2002). However, this region is generally thought of as a downwelling shelf, with onshore Ekman transport resulting from storms generated by the Aleutian Low Pressure system (Weingartner et al., 2005). Previous observations have implicated the wind-generated Ekman transport in the advection of oceanic zooplankton onto the shelf (Cooney, 1986; Coyle et al., 2013). Oceanic zooplankton overwinter in deep water off the shelf, but undergo a vertical migration to occupy surface waters in spring. As such, their early life history has much in common with age-0 sablefish, and we can expect similar transport mechanisms to be in play. For our part, we found a moderate, positive correlation between on-shelf flow in the west-central Gulf and sablefish recruitment. No relationship was found between recruitment and on-shelf advection in the eastern Gulf. Coffin and Mueter (2015) also found recruitment of age-2 individuals to the adult stock to be unrelated to downwelling favorable winds or freshwater discharge (environmental variables they selected as indicators of cross-shelf and along-shelf transport) during the larval and early juvenile phase (age-0) life stage. Our evidence of a potential relationship between recruitment dynamics and regional advective processes suggests that Coffin and Mueter's (2015) advection proxies, which were based on point location data, may have missed some transport processes that were captured by the spatially resolved hydrodynamic model.

The lack of an overwhelming relationship between sablefish recruitment and model derived on-shelf advection (towards nursery sites) is likely due to the modification of on-shelf

Ekman transport by other physical factors. Cross-shelf exchange in the GOA can be influenced by the propagation of eddies that form in the northeastern GOA along the shelf-break (Ladd et al., 2005). The Haida (Mackas and Galbraith, 2002; Whitney and Robert, 2002) and Sitka (Crawford, 2002; Matthews et al., 1992) eddies tend to propagate out into the basin, while the Yakutat eddies (Okkonen et al., 2001) tend to stay close to the shelf-break, so that depending on the eddy field present at the time of sablefish spawning, eddies could be responsible for enhancing or suppressing on-shelf transport of young sablefish. The ROMS model used to drive the IBM produces eddies with approximately the same scale, frequency, and kinetic energy off the northern Gulf of Alaska shelf break as observed (Coyle et al., 2012), but because it does not use any data assimilation, the model eddies are randomly generated features, and their spatial and temporal occurrence in the model does not necessarily coincide with reality. Likewise, the model does not precisely capture other short-term chaotic events, such as storms that track through the region and influence local wind and run-off fields. Gibson et al. (2013) found that, in the Eastern Bering Sea, relatively short (days to weeks) periods of southeasterly wind could significantly impact the transport of oceanic zooplankton onto the shelf. A mismatch in sablefish recruitment and modeled advection, or predicted connectivity, could thus be partially due to dynamical models' inability to simulate the correct timing of these short-term atmospheric and oceanic events. Also, because the sablefish IBM was driven by tidally filtered, daily average flow fields from the ROMS hydrographic model, sub-daily dynamics such as the tidal cycle will also not be captured. Despite the shortcomings of the model, we have shown there is sufficient on-shelf advection to transport young sablefish from off-shelf deep spawning sites over the shelf break to shallow onshore nursery areas, without the inclusion of any horizontal swimming behavior—such as toward food or a particular geographic location.

4.4. Important spawning regions for Alaska sablefish

The northern sablefish population, which inhabits the GOA, is thought to extend south into northern British Columbia (Echave et al., 2013; Kimura et al., 1998). Sablefish are also thought to spawn throughout their range (Kimura et al., 1998), although the prevailing theory for Alaska sablefish is that the majority of the spawners exist in the central and eastern GOA (Funk and Bracken, 1984; Shotwell et al., 2014). Our model simulations suggest that individuals spawned in the east were more likely to be successfully transported to a nursery area *within* the Gulf than individuals spawned in the west; individuals spawned in the western Gulf were generally advected out of our Gulf of Alaska model domain. Sablefish spawned off the coast of Sitka and Cross Sound (alongshore areas 2 and 3) had the highest likelihood of settling. The southeastern-most region in our model domain (alongshore area 1) did produce successful settlers, but to a lesser extent than the regions immediately north, suggesting that individuals spawning here are perhaps less likely to contribute to the Alaska population. Although conventional wisdom is that adult sablefish are spawning in deep water along the continental slope (Mason et al., 1983), as was simulated in our model, small stocks of sablefish have been reported to spawn in some mainland inlets, including Chatham Strait (located in alongshore zone 1; Bracken et al., 1997). Individuals spawning in Chatham Strait have a relatively low movement rate (Hanselman et al., 2014a), and young individuals may be recruited directly to shallow inshore areas within the strait. It is possible that these small, inshore spawning populations that were underrepresented in our model have a disproportionality large impact on the overall recruitment success of GOA sablefish.

4.5. Nursery areas

Our study indicates that, in the absence of any horizontal directional movement, sablefish spawned throughout the Gulf have the highest probability for settlement in nursery areas in the central Gulf (alongshore areas 5-6). While the adult sablefish population center is indeed thought to be in the central GOA (Hanselman et al., 2014b), near-shore waters extending from southeast Alaska to British Columbia are known to be some of the most important nursery grounds for young sablefish (Sasaki, 1985). Juvenile sablefish are found consistently at only one site, St. John Baptist Bay (Rutecki and Varosi, 1997), located in alongshore area 3 (Fig. 1), about 33 km north of Sitka. Our study indicated that, while there was connectivity to nursery sites in alongshore area 1-3, primarily from spawning areas to the south, the probability of connectivity to this region is not particularly high if spawning occurs evenly along the shelf break throughout the Gulf. This supports the hypothesis that spawning is likely more concentrated in areas in the southeast, or perhaps that the known settlement in St. John Baptist Bay is dependent on selective behavioral traits of young sablefish. Given the sensitivity of connectivity predictions to settlement depth, improved criteria for the identification of nursery areas (including substrate type, exposure, dominant vegetation, etc.) would be beneficial.

In our model, we used bathymetric depth to define potential nursery areas along the continental slope. Model sensitivity analysis revealed that changes to the settlement depth criterion had the largest impact on multiple key model outputs. However, the model estimates for relative connectivity between spawning and settlement sites were relatively robust, i.e. although fewer individuals would settle in an alongshore zone as settlement depth is reduced, the relative pattern of connectivity remained similar. Because of the relatively coarse representation of the GOA coastline in a 3-km model, Salisbury Sound (the location of St. John Baptist Bay) and other, highly localized nursery areas are represented by little more than a handful of grid points. As such, it is likely that there were instances of individuals being advected close to the entrance to the Sound, but settlement was not triggered because the settlement depth criterion was not reached. A higher resolution coastal model may be able to better capture fine-scale, near-shore dynamics responsible for transporting individuals toward localized settlement regions, i.e. up through the Sound and into water in which they can settle. In addition to settlement depth, minimum size for transition to the juvenile life stage with the ability to settle and depth preferences for the different life stages were some of the most influential parameters for determining model predictions of connectivity. Observational and laboratory studies that could refine these parameters would be extremely beneficial.

In the model, a large proportion of individuals spawned in alongshore areas 6-9 (central-western Gulf) reached the settlement life-stage but were transported away from the shelf, toward the GOA ocean basin. As the model had no viable habitat for triggering settlement in this region, these individuals were considered ‘unsuccessful.’ This region does, however, have a number of sea mounts where sablefish are known to dominate the groundfish population (Maloney, 2004). Although current thought is that these populations are maintained by the recruitment of larger adult fish from the slope rather than local reproduction (Maloney, 2004), it is worth considering that there is potential for young sablefish spawned on the continental slope to be transported to these seamounts. Whether the surface of the seamounts is shallow enough to trigger settlement, or if the seamounts have other, as yet unknown, habitat criteria remain open questions.

4.6. Relating modeled connectivity to the observed distribution patterns

Doyle and Mier (2015) found sablefish eggs offshore in the western GOA in February. However, in this region, the Alaskan Stream flows westward with speeds averaging 50 cm s^{-1} (Stabeno et al., 2004). Assuming the duration of the egg stage is eleven days (Alderdice et al., 1988; Mcfarlane and Beamish, 1992), eggs observed within the Alaska Stream could have been transported from ~475 km away. While it is possible they could be carried to the western GOA in a countercurrent from farther west, i.e. the Aleutian Islands or from farther offshore, we believe it is most likely these individuals were spawned farther east than where they were sampled, and were carried to the sample location in the prevailing current. A small population of sablefish does exist in the western GOA and Aleutian Islands, but our study indicates that sablefish spawned in this region will probably not settle in nursery areas in the Gulf unless some form of active migration or utilization of fine-scale currents (i.e. localized canyon transport) absent from our 3-km resolution model is implemented by the young individuals.

It is possible that the model domain itself could impact our understanding of connectivity within the Alaska sablefish population, as individuals advected outside of the model domain could potentially still be part of the Alaska stock. Previous modeling studies focused on zooplankton (Gibson et al., 2013) and pollock larvae (Parada et al., 2016) indicate that, rather than being 'lost' to the North Pacific basin, organisms in the western Alaska Stream may enter the Bering Sea via Aleutian Island passes. Thus, it does seem possible that the age-0 sablefish that exited the model domain to the west could settle in nursery areas in the Aleutians or eastern Bering Sea. At 3-4 years old, sablefish are known to move away from their shallow nursery areas into deeper water, and in the GOA at least, individuals eventually undergo a counterclockwise migration as fish age. Most adult fish return eastward by ages 7-9 (Maloney and Sigler, 2008). Thus, individuals that exit the GOA to the west could eventually return and contribute to the GOA sablefish population in greater proportions than the model suggests. It was far less probable for individuals to be advected out of the southeastern model domain and into Canadian waters, so presumable this choice of boundary location has less of an influence on our overall understanding of connectivity.

4.7. Impact of environmental conditions on year-class success

Our sablefish model does not predict the actual recruitment of age-2 sablefish to the population, but we can use our measure of 'Total Connectivity,' or the probability of successfully settling in a nursery area in the Gulf integrated across all spawning areas, as an estimate of likely success of a year-class. 'Total Connectivity' was more closely correlated to variability in the recruitment of sablefish, as determined by the Alaska stock assessment (Hanselmen et al., 2014), than was the overall spatial pattern of connectivity in the Gulf, or the connectivity to more localized regions containing known nursery area, i.e. alongshore area 3, containing known nursery area St. John Baptist Bay. This is in line with the observation that during years of high recruitment, juveniles are widespread in inside waters throughout their migration range (Gao et al., 2004; Maloney and Sigler, 2008; Rutecki and Varosi, 1997). This has been true for the 1959, 1971, 1977, 1980, 1984, 1989, 1991, 1997, and 2000 year-classes, all of which proved to be above average in size (Echave et al., 2013; Hanselman et al., 2014b). The relatively strong year-classes of Alaska sablefish from 1977 through 1988 were during a positive phase of the Pacific Decadal Oscillation (PDO), a regime characterized by strong Aleutian Lows and above-average southwesterly and westerly winds, cooling in the central Subarctic Pacific

and warming along the coast (Hermann et al., 2016; King et al., 2001). Our modeling study covered the relatively short sixteen-year period from 1996 to 2011, during which time the PDO oscillated from positive to negative on a greater then decadal frequency. According to the most recent stock assessment available (Hanselman et al., 2014b), 1997 was a relatively strong year-class, occurring during a positive phase of the PDO, while the other strong year-class during this period (2000) occurred during a negative phase (http://research.jisao.washington.edu/pdo/). Our model predicted that 1997, a year with average salinity but warmer than average temperatures, would have much higher 'Total Connectivity,' and that 2000, a year when the PDO was negative, temperatures were lower, and salinity was higher, would have a connectivity slightly above average.

We did not find any correlation between recruitment and simple physical environmental indices for temperature or salinity predicted by the hydrographic model. King et al. (2000) found that above average recruitment to the Canadian sablefish population occurred in years with intense Aleutian Lows and more frequent southwesterly winds. Schirripa and Colbert (2006) found a significant positive relationship between recruitment to the U.S. West Coast sablefish population and northward and eastward Ekman transport, which would have arisen from easterly and southerly winds. These differences in significant wind direction are not surprising, given the curvature of the coastline. We undertook a preliminary analysis exploring the relationship between wind direction in the eastern and western Gulf of Alaska and the Gulf-wide annual sablefish recruitment (Appendix B). In the eastern Gulf there was a significant, positive correlation between annual sablefish recruitment and south-easterly wind in January-March and southerly wind from January-March and May-July. In the western Gulf, we found a positive correlation between easterly, southerly and southeasterly wind from February-March. The correlation with southeasterly wind continued through April. These correlations are exploratory so should be treated with caution but they do suggest that wind-induced transport may play a role in recruitment success, which warrants further investigation.

Sablefish recruitment success certainly relies not only on successful transport between spawning and nursery areas (connectivity), but on adequate food supply. Sablefish have a very fast growth rate (Sigler et al., 2001), thought to be driven by high consumption, rather than unusually efficient energy transfer (Sogard and Olla, 2001). Sablefish larvae consume mostly copepods (Kendall and Matarese, 1987), and McFarlane and Beamish (1992) concluded that year-class strength in sablefish was related to very early larval survival, which was dependent on copepod production for post-yolk-sac stages during upward migration to surface waters and further coincident with the upward migration of *Neocalanus* naupli (Dagg et al., 2006). Schirripa and Colbert (2006) have suggested that environmental conditions later in the neustonic stage may also play a role in fine-tuning survival. Coffin and Mueter found sablefish recruitment to be positively related to July upwelling-favorable winds during age-1 and age-2, indicating that in the years following transport of age-0 individuals to the nursery area, upwelling winds could have an impact on sablefish success, perhaps due to the increase in nutrients and production this might bring (Ladd et al., 2005). Shotwell et al. (2014) have proposed that a strong year-class of Alaska sablefish relies upon the compounding effects of three separate bio-physical mechanisms: 1) a successful match between the timing of sablefish entering the outer shelf domain and the arrival of productive North Pacific cold-pool waters; 2) increased anticyclonic eddy activity in the mid-shelf domain and entrainment of sablefish in eddies with productive centers; and 3) higher stratification along the coast due to warmer sea-surface temperature and increased freshwater discharge, resulting in an early spring bloom that supports a large zooplankton

biomass. This food-dependent mechanism was not captured directly in the IBM as, in this first iteration, individuals had constant stage-specific growth rates, which were not impacted by food availability. Total connectivity and primary production in both spring and summer had modest positive correlations with recruitment, and the lower trophic level NPZ model predicted both 1997 and 2000 (high recruitment years) to be years with much greater than average primary production. This increased production could have contributed to the recruitment success of these year-classes by supporting increased secondary production that the young sablefish could consume.

Our model assumes that individuals that have not managed to settle in a nursery area by December 31st will not survive. This means that individuals 'spawned' earlier in the year would have a longer time to reach a suitable area. We feel this is a reasonable assumption, as during winter in the Gulf of Alaska there would be very little food available for the young individuals to consume since primary producers are severely light limited at this time (Cooney, 2006). We think it unlikely that individuals that have not settled prior to this time would thrive. We hope that a future version of the model will be able to include explicit feeding by sablefish on zooplankton. The relatively strong relationship between production and recruitment indicated by our correlations suggests that adding explicit feeding and food-dependent metabolic processes would be a worthwhile addition to the sablefish IBM model. This would enable us to better address the question of environmental impacts on production fields, and how this variability aligns with sablefish metabolic demands. Such a model enhancement would require information from field studies regarding the impact of food availability on growth and respiration, because, to date, there is very little information available to support the development of such an algorithm.

Given the interplay of the multiple factors that can affect sablefish, it is perhaps not surprising that no single variable had a very strong correlation with recruitment. Using ordinary linear regression models, we demonstrate that 'Total Connectivity,' annual on-shelf transport in the eastern GOA, and spring and summer primary production can together explain greater than 50 % of the variability in GOA sablefish recruitment between 1996 and 2011. Although this is less than the 70 % of the sablefish recruitment variability explained by Schirripa and Colbert (2006) for the California Current System, De Oliveira and Butterworth (2005) suggest that indices from modeling efforts as measures of 'recruitment' can be considered useful for assessment scientists and fishery managers if the index, or combination of indices, is able to explain >50 % of the variability in past recruitment.

5. Summary and Conclusion

Using a novel IBM for sablefish, we could account for ~20 % of the variability in sablefish recruitment predicted by the assessment model for Alaska-wide stock. Combining IBM model estimates for settlement success with lower trophic level estimates of primary production, we were able to account for up to 50 % of the recruitment variability. Our major findings were that 1) modeling showed that young sablefish settling in nursery areas in the GOA were most likely spawned in the eastern Gulf; 2) sablefish spawning in the western Gulf are unlikely to settle in the GOA and are more likely to be advected farther west, perhaps to settle in the Aleutian islands or Bering Sea (to contribute to the Alaska population, they would have to undergo an active return migration as they mature); 3) "Total Connectivity" between all spawning sites and nursery areas was more strongly correlated to estimates of age-2 recruitment from the stock assessment model for the Alaska-wide stock than the strength of connections to or

from specific regions; and 4) transport to St. John Baptist Bay, a known nursery area, was not the most probable end point for sablefish, if spawning was assumed homogeneous along the continental slope. These latter findings suggest that young individuals arrive at this persistent nursery area due to highly localized spawning, small-scale currents missing in the regional GOA model, or directional movement behavior in young fish.

It is also important to be cognizant of the relatively short time series used in the study (sixteen years), which nevertheless was the longest available time series for output from the computational expensive 3-km model. Extending our analysis to include multiple decades and multiple phases of the PDO would add robustness to our conclusions. The fact that no single corollary from our bio-physical model analysis had a very strong relationship to sablefish recruitment contributes to the conclusion that recruitment variability arises due to complex interactions between the environment and the biology of the individual. Temperature- and food-dependent growth rates not presently captured in the IBM may be important missing factors, as could other environmental pressures (such as predation or competition), to which individuals could be subjected following settlement in a nursery area, but prior to reaching the age at recruitment. Improved criteria for nursery area selection were also identified as a model enhancement that could improve estimates of year-class success.

Our analysis has enabled us to develop a conceptual figure for sablefish transport onto the GOA shelf to shallow nursery areas (Fig. 13). Though the timing and extent for this transport shows significant interannual variability, the location of likely source areas and the comparative strength of the connectivity between spawning and nursery sites appear to be relatively consistent year-to-year. It is important to note that this illustration of the most likely connections assumes that sablefish spawning throughout the Gulf is homogeneous. Future iterations of the sablefish IBM would greatly benefit from collaboration with sablefish stock assessment scientists, in order to better refine likely spawning and nursery areas. Such refinements should increase the model's skill for predicting likely sablefish 'settlement' success. In addition, development of a GOA-specific recruitment index in the stock assessment model, or expansion of the IBM domain to the entire Alaska stock region, would improve the internal consistency of comparisons between recruitment indices from the stock assessment model and settlement indices from the IBM. An enhanced IBM that could skillfully predict age-2 recruitment from settlement of age-0 sablefish would likely be very informative to sablefish stock assessment and management.

Acknowledgements

This work was funded through the North Pacific Research Board-sponsored Gulf of Alaska Integrated Ecosystem Research Program under award #G84. This research represents contribution EcoFOCI-0859 to NOAA's Fisheries-Oceanography Coordinated Investigations, Pacific Marine Environmental Laboratory contribution 4432, and Alaska Fisheries Science Center contribution AFSC-2905. This publication was partially funded by the Joint Institute for the Study of the Atmosphere and Ocean (JISAO) under NOAA Cooperative Agreement NA15OAR4320063, Contribution No. 2018-0143. This work was supported in part by the high-performance computing and data storage resources operated by the Research Computing Systems Group at the University of Alaska Fairbanks, Geophysical Institute. This manuscript is NPRB publication number 669 and Gulf of Alaska Project publication number 27. The authors would like to thank K. Hedstrom for her effort in the initial development of the ROMS Gulf of

Alaska model, upon which our experiments were based, as well as the three anonymous reviewers that provided detailed and thoughtful commentary to improve the clarity of this manuscript. The findings and conclusions in the paper are those of the author(s) and do not necessarily represent the views of the National Marine Fisheries Service. Reference to trade names does not imply endorsement by the National Marine Fisheries Service, NOAA.

References

Alderdice, D.F., Jensen, J.O.T., Velsen, F.P.J., 1988. Preliminary trials on incubation of sablefish eggs. Aquaculture 69, 271–290.

Allen, M.J., Smith, G.B., 1988. Atlas and zoogeography of common fishes in the Bering Sea and northeastern Pacific, U.S. Dept. Commer., NOAA Technical Report NMFS 66, 158 p.

Bailey, K.M., Stabeno, P.J., Powers, D.A., 1997. The role of larval retention and transport features in mortality and potential gene flow of walleye pollock. J. Fish Biol. 51, 135–154.

Bartsch, J., Brander, K., Heath, M., Munk, P., Richardson, K., Svendsen, E., 1989. Modelling the advection of herring larvae in the North Sea. Nature 340, 632–636.

Belkin, I.M., Cornillon, P., Ullman, D., 2003. Ocean Fronts Around Alaska From Satellite SST Data, p. 15, in: Proceedings of the American Meteorological Society 7th Conference on the Polar Meteorology and Oceanography. Hyannis, MA.

Belkin, I.M., Krishfield, R., Honjo, S., 2002. Decadal variability of the North Pacific Polar Front: Subsurface warming versus surface cooling. Geophys. Res. Lett. 29.

Bracken, B.E., Gordon, D.A., Carlile, D.W., 1997. Sablefish, *Anoplopoma fimbria*, Stock Assessment in the Inside Waters of Southeast Alaska, pp. 195–206, in: Wilkins, M.E., Saunders, M.W. (Eds.), Biology and Management of Sablefish, *Anoplopoma fimbria*, U.S. Dept. Commer., NOAA Technical Report NMFS 130, 286 p.

Cheng, W., Hermann, A.J., Coyle, K.O., Dobbins, E.L., Kachel, N.B., Stabeno, P.J., 2012. Macro- and micro-nutrient flux to a highly productive submarine bank in the Gulf of Alaska: A model-based analysis of daily and interannual variability. Prog. Oceanogr. 101, 63–77. doi:DOI 10.1016/j.pocean.2012.01.001

Coffin, B., Mueter, F., 2015. Environmental covariates of sablefish (*Anoplopoma fimbria*) and Pacific ocean perch (*Sebastes alutus*) recruitment in the Gulf of Alaska. Deep-Sea Res. Part II Top. Stud. Oceanogr. doi:10.1016/j.dsr2.2015.02.016

Cooney, R.T., 1986. The seasonal occurrence of *Neocalanus cristatus*, *Neocalanus plumchrus*, and *Eucalanus bungii* over the shelf of the northern Gulf of Alaska. Cont. Shelf Res. 5, 541–553. doi:10.1016/0278-4343(86)90075-0

Cooney, T. 2006.the marine production cycle, pp. 47-59, in: Spies, R.B. (Ed.), Long-term Ecological Change in the Northern Gulf of Alaska, Elsevier, 608 p.

Cooper, D.W., Duffy-Anderson, J.T., Stockhausen, W.T., Cheng, W., 2013. Modeled connectivity between northern rock sole (*Lepidopsetta polyxystra*) spawning and nursery areas in the eastern Bering Sea. J. Sea Res. 84, 2–12. doi:10.1016/j.seares.2012.07.001

Coutré, K. M., Beaudreau, A. H., Malecha, P. W. (2015). Temporal Variation in Diet Composition and Use of Pulsed Resource Subsidies by Juvenile Sablefish. Transactions of the American Fisheries Society, 144(4), 807-819.

Courtney, D., Rutecki, T.L., 2011. Inshore movement and habitat use by juvenile sablefish, *Anoplopoma fimbria*, implanted with acoustic tags in southeast Alaska, AFSC Processed Report 2011-01, 39 p. Alaska Fish. Sci. Cent., NOAA, Natl. Mar, Fish. Serv., Auke Bay

Laboratories,17109 Lena Point Loop Road Juneau, AK 99801.
Coyle, K.O., Cheng, W., Hinckley, S.L., Lessard, E.J., Whitledge, T., Hermann, A.J., Hedstrom, K., 2012. Model and field observations of effects of circulation on the timing and magnitude of nitrate utilization and production on the northern Gulf of Alaska shelf. Progr. Oceanogr. 103, 16–41. doi:10.1016/j.pocean.2012.03.002
Coyle, K.O., Gibson, G. A., Hedstrom, K., Hermann, A. J., Hopcroft, R.R., 2013. Zooplankton biomass, advection and production on the northern Gulf of Alaska shelf from simulations and field observations. J. Mar. Syst. 128, 185–207. doi:10.1016/j.jmarsys.2013.04.018
Crawford, W.R., 2002. Physical characteristics of Haida Eddies. Journal of Oceanography 58 (5), 703–713.Dagg, M.J., Liu, H., Thomas, A. C., 2006. Effects of mesoscale phytoplankton variability on the copepods *Neocalanus flemingeri* and *N. plumchrus* in the coastal Gulf of Alaska. Deep-Sea Res. Part I Oceanogr. Res. Pap. 53, 321–332. doi:10.1016/j.dsr.2005.09.013
Danielson, S., Curchitser, E., Hedstrom, K., Weingartner, T., Stabeno, P., 2011. On ocean and sea ice modes of variability in the Bering Sea. J. Geophys. Res. Ocean. 116, 1–24. doi:10.1029/2011JC007389
De Oliveira, J.A.A., Butterworth, D.S., 2005. Limits to the use of environmental indices to reduce risk and/or increase yield in the South African anchovy fishery. African J. Mar. Sci. 27.
DeCelles, G., Cowles, G., Liu, C., Cadrin, S., 2015. Modeled transport of winter flounder larvae spawned in coastal waters of the Gulf of Maine. Fish. Oceanogr. 24, 430–444. doi:10.1111/fog.12120
Dickson, D. and Baker, M.R., 2016. Introduction to the North Pacific Research Board Gulf of Alaska Integrated Ecosystem Research Program (GOAIERP): Volume I. Deep Sea Research Part II: Topical Studies in Oceanography http://dx.doi.org/10.1016/j.dsr2.2016.08.005
Dobbins, E.L., Hermann, A.J., Stabeno, P., Bond, N. A., Steed, R.C., 2009. Modeled transport of freshwater from a line-source in the coastal Gulf of Alaska. Deep. Res. Part II Top. Stud. Oceanogr. 56, 2409–2426. doi:10.1016/j.dsr2.2009.02.004
Doyle, M.J., Mier, K.L., 2015. Early life history pelagic exposure profiles of selected commercially important fish species in the Gulf of Alaska. Deep-Sea Res. II. doi:10.1016/j.dsr2.2015.06.019
Echave, K., Hanselman, D.H., Maloney, N.E., 2013. Report to Industry on the Alaska Sablefish Tag Program, 1972-2012, U.S. Dept. Commer., NOAA Technical Memorandum NMFS-AFSC-254, 47 pp.
Fissel, B., Dalton, M., Felthoven, R., Garber-Yonts, B., Haynie, A., Kasperski, S., Lee, J., Lew, D., Pfeiffer, L., Seung, C., 2012. Stock Assessment and Fishery Evaluation Report for the Groundfish Fisheries of the Gulf of Alaska and Bering Sea/Aleutian Islands Area: Economic status of the groundfish fisheries off Alaska, 2011, 309 p., http://www.afsc.noaa.gov/REFM/Docs/2012/economic.pdf.
Funk, F., Bracken, B.E., 1984. Status of the Gulf of Alaska Sablefish (*Anoplopoma fimbria*) resource in 1983. Informational Leaflet No. 235. Alaska Department of Fish and Game Division of Commercial Fisheries Juneau, A1aska 55 p.
Gao, Y., Joner, S.H., Svec, R.A., Weinberg, K.L., 2004. Stable isotopic comparison in otoliths of juvenile sablefish (*Anoplopoma fimbria*) from waters off the Washington and Oregon coast. Fish. Res. 68, 351–360. doi:10.1016/j.fishres.2003.11.002

Garavelli, L., Kaplan, D.M., Colas, F., Stotz, W., Yannicelli, B., Lett, C., 2014. Identifying appropriate spatial scales for marine conservation and management using a larval dispersal model: The case of *Concholepas concholepas* (loco) in Chile. Prog. Oceanogr. 124, 42–53. doi:10.1016/j.pocean.2014.03.011

Gibson, G. A., Coyle, K.O., Hedstrom, K., Curchitser, E.N., 2013. A modeling study to explore on-shelf transport of oceanic zooplankton in the Eastern Bering Sea. J. Mar. Syst. 121-122, 47–64. doi:10.1016/j.jmarsys.2013.03.010

Gibson, G.A., Spitz, Y.H., 2011. Impacts of biological parameterization, initial conditions, and environmental forcing on parameter sensitivity and uncertainty in a marine ecosystem model for the Bering Sea. J. Mar. Syst. 88, 214–231. doi:10.1016/j.jmarsys.2011.04.008

Haidvogel, D.B., Arango, H., Budgell, W.P., Cornuelle, B.D., Curchitser, E., Di Lorenzo, E., Fennel, K., Geyer, W.R., Hermann, A. J., Lanerolle, L., Levin, J., McWilliams, J.C., Miller, A. J., Moore, A. M., Powell, T.M., Shchepetkin, A. F., Sherwood, C.R., Signell, R.P., Warner, J.C., Wilkin, J., 2008. Ocean forecasting in terrain-following coordinates: Formulation and skill assessment of the Regional Ocean Modeling System. J. Comput. Phys. 227, 3595–3624. doi:10.1016/j.jcp.2007.06.016

Hanselman, D.H., Heifetz, J., Echave, K.B., Dressel, S.C., 2014a. Move it or lose it : movement and mortality of sablefish tagged in Alaska. Can. J. Fish. Aquat. Sci. 72(2), , 238–251. doi:10.1139/cjfas-2014-0251

Hanselman, D.H., Lunsford, C.R., Rodgveller, C.J., 2014b. Assessment of the sablefish stock in Alaska, in: Stock Assessment and Fishery Evaluation Report for the Groundfish Resources of the Gulf of Alaska. North Pacific Fishery Management Council, 605W. 4th Avenue, Suite 306, Anchorage, AK 99501, pp. 576–717.

Hart, J.L., 1973. Pacific fishes of Canada. Bull. Fish. Res. Bd. Can. 180, 740 p.

Heifetz, J., Fujioka, J.T., 1991. Movement dynamics of tagged sablefish in the northeastern Pacific 11, 355–374.

Hermann, A.J., Hinckley, S., Dobbins, E.L., Haidvogel, D.B., Bond, N.A., Mordy, C., Kachel, N., Stabeno, P.J., 2009. Deep-Sea Research II Quantifying cross-shelf and vertical nutrient flux in the Coastal Gulf of Alaska with a spatially nested , coupled biophysical model. Deep-Sea Res. Part II 56, 2474–2486. doi:10.1016/j.dsr2.2009.02.008

Hermann, A.J., Ladd, C., Cheng, W., Curchitser, E., Hedstrom, K., 2016. A model-based examination of multivariate physical modes in the Gulf of Alaska. Deep. Res. II.

Hinckley, S., Coyle, K.O., Gibson, G., Hermann, A. J., Dobbins, E.L., 2009. A biophysical NPZ model with iron for the Gulf of Alaska: Reproducing the differences between an oceanic HNLC ecosystem and a classical northern temperate shelf ecosystem. Deep-Sea Res. Part II Top. Stud. Oceanogr. 56, 2520–2536. doi:10.1016/j.dsr2.2009.03.003

Hinckley, S., Hermann, A.J., Megrey, B.A., 1996. Development of a spatially explicit, individual-based model of marine fish early life history. Mar. Ecol. Prog. Ser. 139, 47–68.

Hinckley, S.L., Parada, C., Horne, J.K., Mazur, M.M., Woillez, M., accepted. Comparison of individual-based model output to data using a model of walleye pollock early life history in the Gulf of Alaska. Deep-Sea Res. II.

Hunter, J.R., Macewicz, B.J., Kimbrell, C. A., 1989. Fecundity and other aspects of the reproduction of sablefish, Anoplopoma fimbria, in central California waters. CalCOFI Rep 30, 61–72.

Janout, M. A., Weingartner, T.J., Okkonen, S.R., Whitledge, T.E., Musgrave, D.L., 2009. Some characteristics of Yakutat Eddies propagating along the continental slope of the northern

Gulf of Alaska. Deep-Sea Res. Part II Top. Stud. Oceanogr. 56, 2444–2459. doi:10.1016/j.dsr2.2009.02.006
Kaihatu, J.M., Handler, R. A., Marmorino, G.O., Shay, L.K., 1998. Empirical orthogonal function analysis of ocean surface currents using complex and real-vector methods. J. Atmos. Ocean. Technol. 15, 927–941. doi:10.1175/1520-0426(1998)015<0927:EOFAOO>2.0.CO;2
Kendall, A.W., Matarese, A., 1987. Biology of eggs , larvae , and epipelagic juveniles of sablefish , *Anoplopoma fimbria*, in relation to their potential use in management 49, 1–13.
Kim, J.J., Stockhausen, W., Kim, S., Cho, Y.-K., Seo, G.-H., Lee, J.-S., 2015. Understanding interannual variability in the distribution of, and transport processes affecting, the early life stages of *Todarodes pacificus* using behavioral-hydrodynamic modeling approaches. Progr. Oceanogr. 138(B): 571-583. doi:10.1016/j.pocean.2015.04.003
Kimura, D.K., Shimada, A.M., Shaw, F.R., 1998. Stock structure and movement of tagged sablefish, *Anoplopoma fimbria*, in offshore northeast Pacific waters and the effects of El Niño-Southern Oscillation on migration and growth. Fish. Bull. 96: 42-481.
King, J.R., McFarlane, G., Beamish, R.., 2001. Incorporating the dynamics of marine systems into the stock assessment and management of sablefish. Progr. Oceanogr. 49, 619–639. doi:10.1016/S0079-6611(01)00044-1
Kodolov, L.., 1968. Reproduction of the sablefish (*Anoplopoma fimbria* [Pall.]). Probl. Ichthyol. 8, 531–535.
Krieger, K.J., 1997. Sablefish, *Anoplopoma fimbria*, observed from a manned submersible, in: Wilkins, M.E., Saunders, M.. (Eds.), Biology and Management of Sablefish, *Anoplopoma fimbria*, U.S. Dept. Commer., NOAA Technical Report NMFS 130, pp. 39–43.
Ladd, C., Stabeno, P., Cokelet, E.D., 2005. A note on cross-shelf exchange in the northern Gulf of Alaska. Deep-Sea Res. Part II Top. Stud. Oceanogr. 52, 667–679. doi:10.1016/j.dsr2.2004.12.022
Ladd, C., Stabeno, P.J., 2009. Freshwater transport from the Pacific to the Bering Sea through Amukta Pass. Geophys. Res. Lett. 36, L14608. doi:10.1029/2009GL039095
Leys, C. Ley, C. Klein, O., Bernard, P. Licata, L. 2013. Detecting outliers: Do not use standard deviation around the mean, use absolute deviation around the median. Journal of Experimental Social Psychology. 49, 764-766.
Mackas, D.L., Galbraith, M.D., 2002. Zooplankton distribution and dynamics in a North Pacific eddy of coastal origin: 1. Transport and loss of continental margin species. Journal of Oceanography 58 (5), 725–738.Macewicz, B.J., Hunter, J.R., 1994. Fecundity of sablefish , *Anoplopoma Fimbria*, from Oregon coastal waters. Calif. Coop. Ocean. Fish. Investig. Report 35, 160 – 174.
Maloney, N.E., 2004. Sablefish, *Anoplopoma fimbria*, populations on Gulf of Alaska seamounts. Mar. Fish. Rev. 66, 1–12.
Maloney, N.E., Sigler, M.F., 2008. Age-specific movement patterns of sablefish (*Anoplopoma fimbria*) in Alaska. Fish. Bull. 106, 305–316.
Mason, J.C., Beamish, R.J., McFarlane, G.A., 1983. Sexual maturity, fecundity, and early life history of sablefish (*Anoplopoma fimbria*) off the Pacific Coast of Canada. Can. J. Fish. Aquat. Sci. 40, 2126–2134.
Matthews, P.E., Johnson, M.A., Obrien, J.J., 1992. Observation of mesoscale ocean features in the Northeast Pacific using Geosat radar altimetry data. Journal of Geophysical Research—Oceans 97 (C11), 17829–17840.McDevitt, S. A. 1986. A summary of sablefish catches in

the northeast Pacific Ocean, 1956-84. In US Dep. Commer., NOAA Technical Memorandum NMFSF/NWC-101, p. 34. National Oceanic and Atmospheric Administration, National Marine Fisheries Service, Northwest and Alaska Fisheries Center.McFarlane, G.A., Beamish, R.J., 1992. Climate influence linking copepod produdion with strong year classes in sablefish, Anoplopoma fimbria. Can. J. Fish. Aquat. Sci. 49, 743–753.

McFarlane, G.A., Beamish, R.J., 1983. Biology of adult sablefish (Anoplopoma fimbria) in waters off western Canada. Proc. 2nd Lowell Wakef. Int. Sablefish Symp. Alaska Sea Grant 83, 59–80.

Megrey, B.A., Hinckley, S., 2001. Effect of turbulence on feeding of larval fishes: a sensitivity analysis using an individual-based model. ICES J. Mar. Sci. 58, 1015–1029. doi:10.1006/jmsc.2001.1104

Mueter, F.J., Shotwell, S.K., Atkinson, S., Coffin, B., Doyle, M., Hinckley, S., Rand, K., Waite, J. 2016. Gulf of Alaska Retrospective Data Analysis. North Pacific Research Board, Gulf of Alaska Integrated Ecosystem Research Program, Retrospective Component Final Report

Moore, J.K., Doney, S.C., Lindsay, K., 2004. Upper ocean ecosystem dynamics and iron cycling in a global three-dimensional model. Global Biogeochem. Cycles 18, n/a–n/a. doi:10.1029/2004GB002220

Moser, H.G., Charter, R.L., Smith, P.E., Lo, N.C.H., Ambrose, D. A., Meyer, C. A., Sandknop, E.M., Watson, W., 1994. Early life history of sablefish, *Anoplopoma fimbria*, off Washington, Oregon, and California, With application to biomass estimation. Calif. Coop. Ocean. Fish. Investig. Report 35, 144–159.

NMFS, 2014. Annual Sablefish Estimated Ex-Vessel Prices, 1992 - 2013. https://alaskafisheries.noaa.gov/fisheries-data-reports.

North, E., Schlag, Z., Hood, R., Li, M., Zhong, L., Gross, T., Kennedy, V., 2008. Vertical swimming behavior influences the dispersal of simulated oyster larvae in a coupled particle-tracking and hydrodynamic model of Chesapeake Bay. Mar. Ecol. Prog. Ser. 359, 99–115. doi:10.3354/meps07317

OCSEAP (Outer Continental Shelf Environmental Assessment Program). 1986. Marine fisheries: resources and environments. In D.W. Hood and S.T. Zimmerman leds.l, The Gulf of Alaska: physical environment and biological resources. p. 417- 458. Minerals Manage. Serv. MMS 86-0095, Anchorage, AK.

Okkonen, S.R., Jacobs, G.A., Metzger, E.J., Hurlburt, H.E., Shriver, J.F., 2001. Mesoscale variability in the boundary currents of the Alaska Gyre. Continental Shelf Research 21 (11–12), 1219–1236.

Okkonen, S.R., 2003. Satellite and hydrographic observations of eddy-induced shelf-slope exchange in the northwestern Gulf of Alaska. J. Geophys. Res. 108, 3033. doi:10.1029/2002JC001342

Parada, C., Hinckley, S.L., Horne, J.K., Mazur, M.M., Dorn, M., Hermann, A.J., Curchitser, E.N., 2016. Modeling connectivity of walleye pollock in the Gulf of Alaska: Are there any linkages to Bering Sea and Aleutian Islands? Deep-Sea Research II. 132, 227–239. http://dx.doi.org/10.1016/j.dsr2.2015.12.010

Reed, R.K., 1984. Flow of the Alaskan Stream and its variations. Deep-Sea Res. II. 31, 369–386.

Royer, T.C., 1998. Coastal Processes in the northern North Pacific., pp. 395–413, in: Robinson, A.R., Brink, K.H. (Eds.), The Sea. Wiley, New York.

Royer, T.C., 1982. Coastal fresh water discharge in the northeast Pacific. J. Geophys. Res. 87,

2017. doi:10.1029/JC087iC03p02017
Rutecki, T.L., Varosi, E.R., 1997. Distribution, age, and growth of juvenile sablefish, *Anoplopoma fimbria*, in the Gulf of Alaska, pp. 55–63, in: Wilkins, M.E., Saunders, M.W. (eds.), Biology and Management of Sablefish, *Anoplopoma fimbria*. U.S. Dep. Commer., NOAA Technical Report NMFS-130, 286 p.
Saha, S., Moorthi, S., Wu, X., Wang, J., Nadiga, S., Tripp, P., Behringer, D., Hou, Y.-T., Chuang, H., Iredell, M., Ek, M., Meng, J., Yang, R., Mendez, M.P., van den Dool, H., Zhang, Q., Wang, W., Chen, M., Becker, E., 2014. The NCEP Climate Forecast System Version 2. J. Clim. 27, 2185–2208. doi:10.1175/JCLI-D-12-00823.1
Sasaki, T., 1985. Studies on the sablefish resources of the North Pacific Ocean. Bull. Far Seas Fish. Res. Lab. 22, 107.
Schirripa, M.J., Colbert, J.J., 2006. Interannual changes in sablefish (*Anoplopoma fimbria*) recruitment in relation to oceanographic conditions within the California Current System. Fish. Oceanogr. 15, 25–36. doi:10.1111/j.1365-2419.2005.00352.x
Schumacher, J., Reed, D.R.L., 1987. Physical oceanography, in: Hood, D.W., Zimmerman, S.T. (Eds.), The Gulf of Alaska: Physical Chemical and Biological Resources. National Oceanic and Atmospheric Administration. Washington, D.C., p. 655 pages.
Shchepetkin, A.F., McWilliams, J.C., 2005. The regional oceanic modeling system (ROMS): a split-explicit, free-surface, topography-following-coordinate oceanic model. Ocean Model. 9, 347–404. doi:10.1016/j.ocemod.2004.08.002
Shotwell, S.K., Hanselman, D.H., Belkin, I.M., 2014. Toward biophysical synergy: Investigating advection along the Polar Front to identify factors influencing Alaska sablefish recruitment. Deep-Sea Res. Part II Top. Stud. Oceanogr. 107, 40–53. doi:10.1016/j.dsr2.2012.08.024
Sigler, M.F., Rutecki, T.L., Courtney, D.L., Karinen, J.F., Yang, M.-S., 2001. Young of the year sablefish abundance, growth, and diet in the Gulf of Alaska. Alaska Fish. Res. Bull. 8, 57–70.
Sogard, S., Olla, B., 2001. Growth and behavioral responses to elevated temperatures by juvenile sablefish *Anoplopoma fimbria* and the interactive role of food availability. Mar. Ecol. Prog. Ser. 217, 121–134. doi:10.3354/meps217121
Sogard, S.M., Olla, B.L., 1998. Behavior of juvenile sablefish, *Anoplopoma fimbria* (Pallas), in a thermal gradient: balancing food and temperature requirements. J. Exp. Mar. Bio. Ecol. 222, 43–58.
Stabeno, P.J., Bell, S., Cheng, W., Danielson, S., Kachel, N.B., Mordy, C.W., 2016. Long-term observations of Alaska Coastal Current in the northern Gulf of Alaska. Deep. Res. II.
Stabeno, P.J., Bond, N. A., Hermann, A. J., Kachel, N.B., Mordy, C.W., Overland, J.E., 2004. Meteorology and oceanography of the Northern Gulf of Alaska, Cont Shelf Res. doi:10.1016/j.csr.2004.02.007
Stabeno, P.J., Bond, N.A., Kachel, N.B., Ladd, C., Mordy, C., Strom, S.L., 2016. Southeast Alaskan shelf from southern tip of Baranof Island to Kayak Island: Currents, mixing and chlorophyll-a. Deep. Res. II. 132, 6-23.
Stabeno, P.J., Reed, R.K., Schumacher, J.D., 1995. The Alaska Coastal Current: Continuity of transport and forcing. J. Geophys. Res. 100, 2477–2485.
Stockhausen, W.T., Coyle, K.O., Hermann, A.J., Blood, D., Doyle, M., Gibson, G.A., Hinckley, S. Ladd, C. Parada, C. This Issue. Running the Gauntlet: Connectivity between natal and nursery areas for arrowtooth flounder (Atheresthes stomias)in the Gulf of Alaska, as inferred from a biophysical Individual-based Model. Deep Sea Research II.

Takeshige, A., Miyake, Y., Nakata, H., Kitagawa, T., Kimura, S., 2015. Simulation of the impact of climate change on the egg and larval transport of Japanese anchovy (*Engraulis japonicus*) off Kyushu Island, the western coast of Japan. Fish. Oceanogr. 24, 445–462. doi:10.1111/fog.12121

Verbeeck, H., Samson, R., Verdonck, F., Lemeur, R., 2006. Parameter sensitivity and uncertainty of the forest carbon flux model FORUG: a Monte Carlo analysis. Tree Physiol. 26, 807–17.

Wang, Z., Bovik, A.C., 2009. Love It or Leave It ? IEEE Signal Process. Mag. 26, 98–117. doi:10.1109/MSP.2008.930649

Weingartner, T.J., Danielson, S.L., Royer, T.C., 2005. Freshwater variability and predictability in the Alaska Coastal Current. Deep-Sea Res. Part II Top. Stud. Oceanogr. 52, 169–191. doi:10.1016/j.dsr2.2004.09.030

Werner, F.E., Page, F.H., Lynch, D.R., Loder, J.W., Louch, G.R., Perry, R.I., Greenberg, D. A., Sinclair, M., 1993. Influences of mean advection and simple behavior on the distribution of cod and haddock early life stages on Georges Bank. Fish. Oceanogr. 2, 43–64. doi:10.1111/j.1365-2419.1993.tb00120.x

Werner, F.E., Quinlan, J. A, Lough, R.G., Lynch, D.R., 2001. Spatially-explicit individual based modeling of marine populations: a review of the advances in the 1990s. Sarsia 86, 411–421. doi:10.1080/00364827.2001.10420483

Whitney, F., Robert, M., 2002. Structure of Haida eddies and their transport of nutrient from coastal margins into the NE Pacific Ocean. Journal of Oceanography 58 (5), 715–723.Wing, B.L., Kamikawa, D.J., 1995. Distribution of neustonic sablefish larvae and associated ichthyoplankton in the eastern Gulf of Alaska , May 1990. U.S. Dept. Commer., NOAA Technical Memorandum NMFS-AFSC-53, 48 p.

Wolotira, R.J.J., Sample, T.M., Noel, S.F., Iten, C.R., 1993. Geographic and bathymetric distributions for many commercially important fishes and shellfishes off the west coast of North America, based on research survey and commercial catch data, 1912-1984. U.S. Dept. Commer., NOAA Technical Memorandum NMFS-AFSC-6, 184 p.

Figure Captions

Fig. 1. Geographic model setting and analysis regions in the Gulf of Alaska. Figure includes the outer boundaries of the ROMS model domain, and the twelve alongshore zones and assumed spawning region (500-2000 m isobath) used in the connectivity study. The eastern offshore region used to calculate primary production index from the GOA-NPZ model is also shown (solid black line). PWS = Prince William Sound; PWI = Prince of Wales Island; EBS = Eastern Bering Sea.

Fig. 2. Conceptual view (not to scale) of the sablefish individual-based-model, illustrating the life stages, assumed depth preferences, and rules determining progression from one life stage to the next. Movement from offshore spawning sites to inshore nursery sites is passive and dependent on advection. Inset figure shows a late-stage sablefish larvae (SL 33 mm) reproduced from Kendall and Matarese (1987). Black diamonds represent stage transition and associated rules for transition.

Fig. 3. a) Sablefish spawning dates and weighting applied to results from connectivity analysis. Grey bars indicate the five egg release times used in the simulations—February 20, March 5, March 20, April 5, and June 5. The weighting applied to results from each simulation was computed using egg abundance climatology (Doyle and Mier, 2015). Note that despite extensive sampling in the second half of April and throughout May, no eggs have been found during this time period. b) Schematic to illustrate vertical distribution of egg release depths over the continental shelf, c) Impact of spatial resolution on the probability of individuals released in spawning zone 2 settling in each alongshore nursery; all eggs in the spatial sensitivity analysis were released on February 20, 2003.

Fig. 4. Spatial Similarity Index (SSIM) for several perturbations (b-f) of the reference matrix (a). In each perturbation, the total connectivity between spawning and nursery areas remains the same when summed over the entire matrix, but the connectivity has been dispersed or shifted away from the original diagonal—i.e., b) shows an overall diffusion of connectivity along the diagonal to adjacent cells, whereas c) shows a complete shift of the 'diagonal' connectivity pattern

Fig. 5. a) standardized log-recruitment estimates for sablefish for 1959-2014. Age-2 recruitment estimates correspond to the year in which sablefish are first included in the stock assessment model; b) standardized log-recruitment estimates for sablefish for the 1996-2011 study period. Note that the recruitment time series has been shifted back by two years, such that age-0 recruitment estimates correspond to the year individuals were spawned.

Fig. 6. Fractions of individuals from each spawning area settling in any nursery area within the model domain, integrated over the sixteen-year period. * indicates data outlier.

Fig. 7. Connectivity matrix showing the median probability that individuals released as eggs in each alongshore spawning area successfully settled in (a) each alongshore nursery area, and (b) the associated deviation about the median. c) Boxplots showing the probability of individuals released in each spawning area developing through the settlement stage but advected to the deep ocean basin. The annual connectivity for each year was computed at the end of the simulation on December 31, and the median was computed from annual averages for each of the sixteen years simulated (1996-2011).

Fig. 8. Annual connectivity matrix showing the probability that individuals released as eggs in each alongshore spawning area successfully settled in each alongshore nursery area for the

years 1996-2011. The connectivity for each year was computed at the end of the simulation on December 31.

Fig. 9. First (a) and second (b) mode spatial patterns from an EOF analysis of the annual mean probability of connection between the spawning area- nursery area pairs across the GOA for the 1996-2011period.The corresponding 1st (black) and 2nd (grey) principal component time-series (PC) are shown in (c).

Fig. 10. Standardized indices (a-e) from the 3 km GOA model and the IBM, and their correlations with recruitment (ai-ei). a) Total fraction settled of all individuals spawned (C_{TOT}); b) fraction recruiting from spawning area 1 (C_{s1}, grey markers) and fraction recruiting to nursery area 3 (C_{n3}, black markers); c) Structural Similarity Index (SSIM); d) 1st Principal Component (PC1, black markers) and 2nd Principal component (PC2, grey markers); and e) Spring Primary Production eastern offshore region (PP_{SprR5}) and Summer Primary Production eastern onshore region (PP_{SumR4}).

Fig. 11. Connectivity matrix for 2002 showing the median probability that individuals released as eggs in each alongshore spawning area successfully settled in each alongshore nursery area (a), and the associated deviation about the median (b). The connectivity for each year was computed at the end of the simulation on December 31. This analysis comprised 500 simulations, in which the values for 37 parameters were drawn randomly from defined probability distributions. All eggs were released on February 20, 2002. See Methods for additional details.

Fig. 12. Connectivity matrix showing the scaled median probability that individuals released as eggs in each alongshore spawning area successfully settled in each alongshore nursery area for a settlement depth criteria of a) 15 m, b) 20 m, c) 50 m, and d) 100 m. All eggs in the spatial sensitivity analysis were released on February 20, 2002. Each matrix was scaled by its maximum connectivity value, such that all values range from 0-1.

Fig. 13. Schematics of likely connections from alongshore spawning areas to alongshore nursery areas. Arrows do not indicate the path of travel. a) Strongest connections, from spawning areas 2-3; (b) probable connections from areas 4-5 to 8-9 (black), from areas 3-6 to 8-9 (dotted), and from areas 1 to 4-6 (white); and c) most likely source location for individuals settling in area 3 to St. John Baptist Bay.

Figure Captions

Fig. 1. Geographic model setting and analysis regions in the Gulf of Alaska. Figure includes the outer boundaries of the ROMS model domain, and the twelve alongshore zones and assumed spawning region (500-2000 m isobath) used in the connectivity study. The eastern offshore region used to calculate primary production index from the GOA-NPZ model is also shown (solid black line). PWS = Prince William Sound; PWI = Prince of Wales Island; EBS = Eastern Bering Sea.

Fig. 2. Conceptual view (not to scale) of the sablefish individual-based-model, illustrating the life stages, assumed depth preferences, and rules determining progression from one life stage to the next. Movement from offshore spawning sites to inshore nursery sites is passive and dependent on advection. Inset figure shows a late-stage sablefish larvae (SL 33 mm) reproduced from Kendall and Matarese (1987). Black diamonds represent stage transition and associated rules for transition.

Fig. 3. a) Sablefish spawning dates and weighting applied to results from connectivity analysis. Grey bars indicate the five egg release times used in the simulations—February 20, March 5, March 20, April 5, and June 5. The weighting applied to results from each simulation was computed using egg abundance climatology (Doyle and Mier, 2015). Note that despite extensive sampling in the second half of April and throughout May, no eggs have been found during this time period. b) Schematic to illustrate vertical distribution of egg release depths over the continental shelf, c) Impact of spatial resolution on the probability of individuals released in spawning zone 2 settling in each alongshore nursery; all eggs in the spatial sensitivity analysis were released on February 20, 2003.

Fig. 4. Spatial Similarity Index (SSIM) for several perturbations (b-f) of the reference matrix (a). In each perturbation, the total connectivity between spawning and nursery areas remains the same when summed over the entire matrix, but the connectivity has been dispersed or shifted away from the original diagonal—i.e., b) shows an overall diffusion of connectivity along the diagonal to adjacent cells, whereas c) shows a complete shift of the 'diagonal' connectivity pattern

Fig. 5. a) standardized log-recruitment estimates for sablefish for 1959-2014. Age-2 recruitment estimates correspond to the year in which sablefish are first included in the stock assessment model; b) standardized log-recruitment estimates for sablefish for the 1996-2011 study period. Note that the recruitment time series has been shifted back by two years, such that age-0 recruitment estimates correspond to the year individuals were spawned.

Fig. 6. Fractions of individuals from each spawning area settling in any nursery area within the model domain, integrated over the sixteen-year period. * indicates data outlier.

Fig. 7. Connectivity matrix showing the median probability that individuals released as eggs in each alongshore spawning area successfully settled in (a) each alongshore nursery area, and (b) the associated deviation about the median. c) Boxplots showing the probability of individuals released in each spawning area developing through the settlement stage but advected to the deep ocean basin. The annual connectivity for each year was computed at the end of the simulation on December 31, and the median was computed from annual averages for each of the sixteen years simulated (1996-2011).

Fig. 8. Annual connectivity matrix showing the probability that individuals released as eggs in each alongshore spawning area successfully settled in each alongshore nursery area for the

years 1996-2011. The connectivity for each year was computed at the end of the simulation on December 31.

Fig. 9. First (a) and second (b) mode spatial patterns from an EOF analysis of the annual mean probability of connection between the spawning area- nursery area pairs across the GOA for the 1996-2011period.The corresponding 1st (black) and 2nd (grey) principal component time-series (PC) are shown in (c).

Fig. 10. Standardized indices (a-e) from the 3 km GOA model and the IBM, and their correlations with recruitment (ai-ei). a) Total fraction settled of all individuals spawned (C_{TOT}); b) fraction recruiting from spawning area 1 (C_{s1}, grey markers) and fraction recruiting to nursery area 3 (C_{n3}, black markers); c) Structural Similarity Index (SSIM); d) 1st Principal Component (PC1, black markers) and 2nd Principal component (PC2, grey markers); and e) Spring Primary Production eastern offshore region (PP_{SprR5}) and Summer Primary Production eastern onshore region (PP_{SumR4}).

Fig. 11. Connectivity matrix for 2002 showing the median probability that individuals released as eggs in each alongshore spawning area successfully settled in each alongshore nursery area (a), and the associated deviation about the median (b). The connectivity for each year was computed at the end of the simulation on December 31. This analysis comprised 500 simulations, in which the values for 37 parameters were drawn randomly from defined probability distributions. All eggs were released on February 20, 2002. See Methods for additional details.

Fig. 12. Connectivity matrix showing the scaled median probability that individuals released as eggs in each alongshore spawning area successfully settled in each alongshore nursery area for a settlement depth criteria of a) 15 m, b) 20 m, c) 50 m, and d) 100 m. All eggs in the spatial sensitivity analysis were released on February 20, 2002. Each matrix was scaled by its maximum connectivity value, such that all values range from 0-1.

Fig. 13. Schematics of likely connections from alongshore spawning areas to alongshore nursery areas. Arrows do not indicate the path of travel. a) Strongest connections, from spawning areas 2-3; (b) probable connections from areas 4-5 to 8-9 (black), from areas 3-6 to 8-9 (dotted), and from areas 1 to 4-6 (white); and c) most likely source location for individuals settling in area 3 to St. John Baptist Bay.

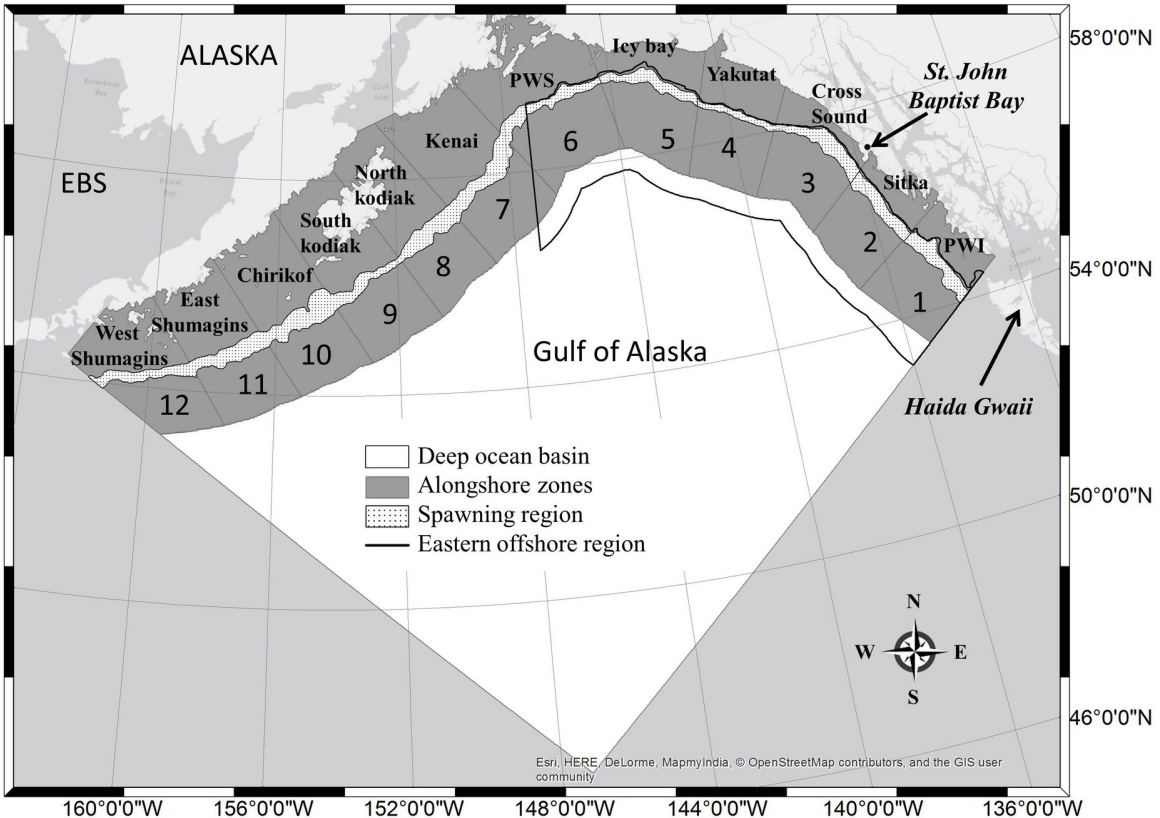
ALASKA
EBS
Icy bay
PWS
Yakutat
Cross Sound
St. John Baptist Bay
Kenai
North kodiak
South kodiak
Chirikof
East Shumagins
West Shumagins
Sitka
PWI
Haida Gwaii
Gulf of Alaska
1
2
3
4
5
6
7
8
9
10
11
12
Deep ocean basin
Alongshore zones
Spawning region
Eastern offshore region
N
W
E
S
58°0'0"N
54°0'0"N
50°0'0"N
46°0'0"N
160°0'0"W
156°0'0"W
152°0'0"W
148°0'0"W
144°0'0"W
140°0'0"W
136°0'0"W
Esri, HERE, DeLorme, MapmyIndia, © OpenStreetMap contributors, and the GIS user community

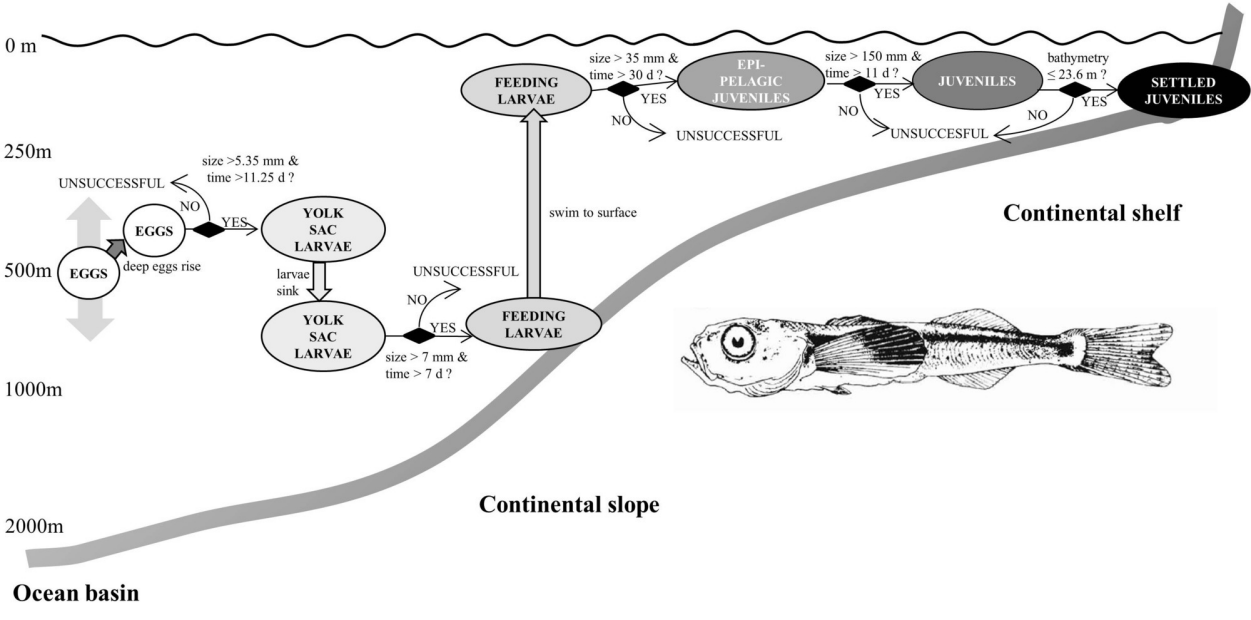
0 m
250m
500m
1000m
2000m
EGGS
deep eggs rise
EGGS
NO
YES
UNSUCCESSFUL
size >5.35 mm &
time >11.25 d ?
YOLK
SAC
LARVAE
larvae
sink
YOLK
SAC
LARVAE
NO
YES
UNSUCCESSFUL
size > 7 mm &
time > 7 d ?
FEEDING
LARVAE
swim to surface
FEEDING
LARVAE
size > 35 mm &
time > 30 d ?
YES
NO
UNSUCCESSFUL
EPI-
PELAGIC
JUVENILES
size > 150 mm &
time > 11 d ?
YES
NO
UNSUCCESSFUL
JUVENILES
bathymetry
≤ 23.6 m ?
YES
NO
SETTLED
JUVENILES
Continental shelf
Continental slope
Ocean basin

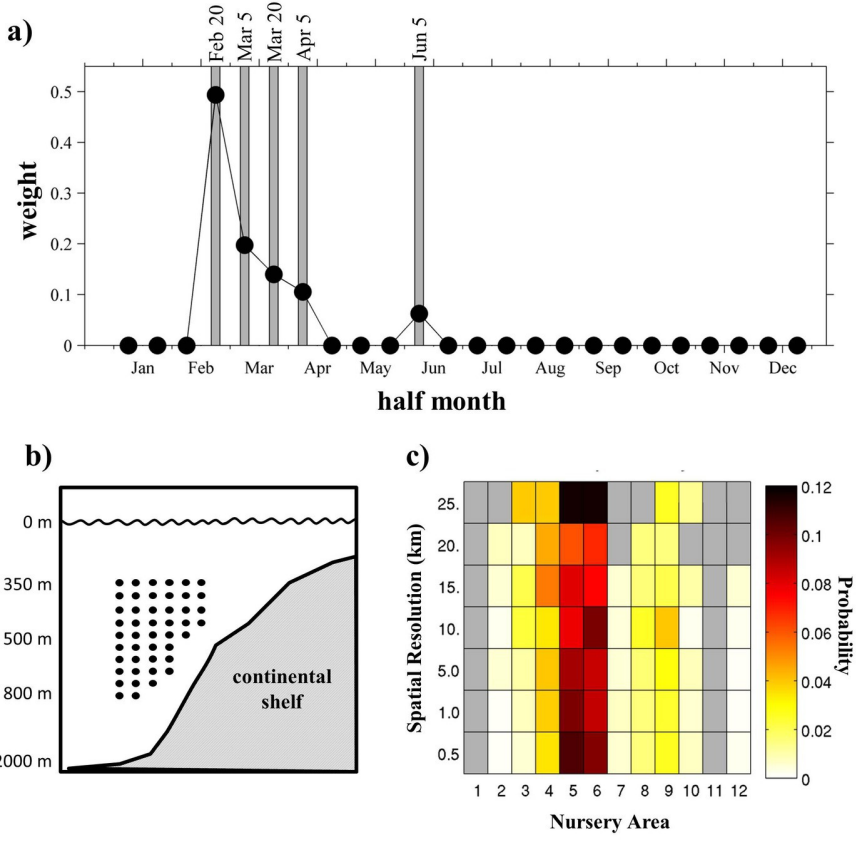
a)
Feb 20
Mar 5
Mar 20
Apr 5
Jun 5
weight
0.5
0.4
0.3
0.2
0.1
0
Jan
Feb
Mar
Apr
May
Jun
Jul
Aug
Sep
Oct
Nov
Dec
half month
b)
0 m
350 m
500 m
800 m
2000 m
continental
shelf
c)
Spatial Resolution (km)
25.
20.
15.
10.
5.0
1.0
0.5
1 2 3 4 5 6 7 8 9 10 11 12
Nursery Area
0.12
0.1
0.08
0.06
0.04
0.02
0
Probability

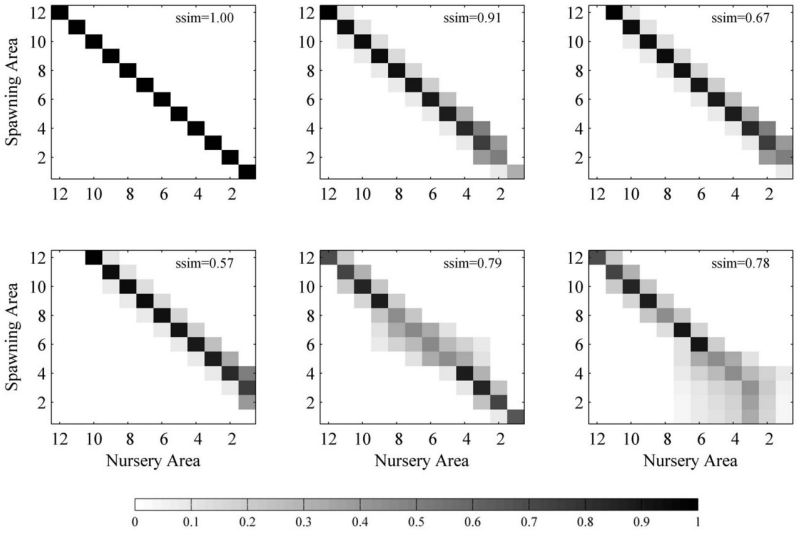
ssim=1.00
ssim=0.91
ssim=0.67
ssim=0.57
ssim=0.79
ssim=0.78
Spawning Area
Spawning Area
Nursery Area
Nursery Area
Nursery Area
12 10 8 6 4 2
0 0.1 0.2 0.3 0.4 0.5 0.6 0.7 0.8 0.9 1

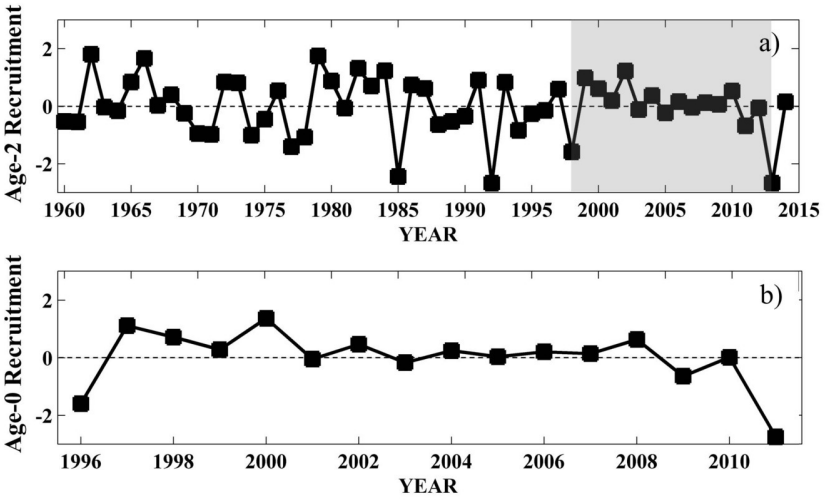
Age-2 Recruitment
a)
2
0
-2
1960
1965
1970
1975
1980
1985
1990
1995
2000
2005
2010
2015
YEAR
Age-0 Recruitment
b)
2
0
-2
1996
1998
2000
2002
2004
2006
2008
2010
YEAR

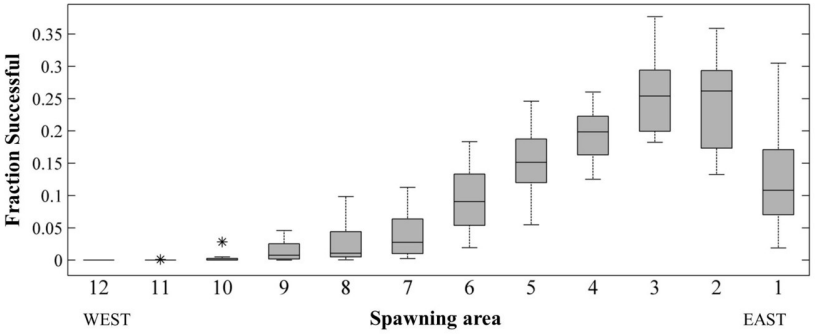
Fraction Successful
0.35
0.3
0.25
0.2
0.15
0.1
0.05
0
12
11
10
9
8
7
6
5
4
3
2
1
WEST
Spawning area
EAST

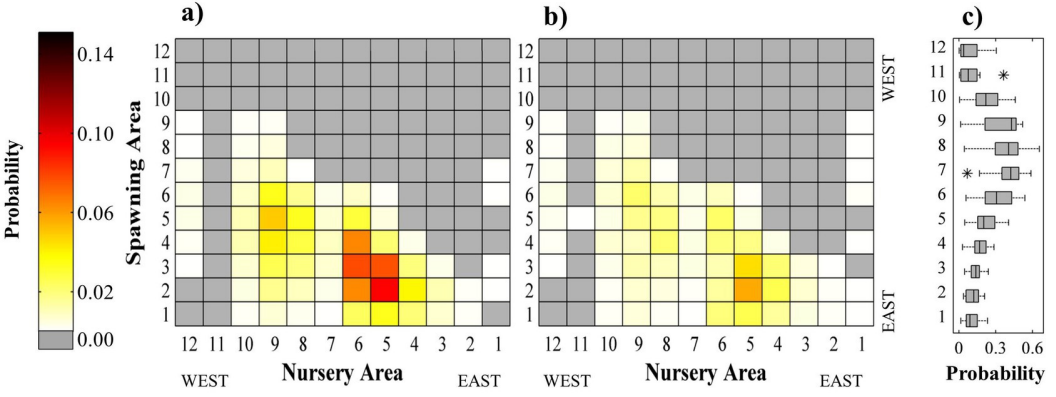
a)
b)
c)
Probability
0.14
0.10
0.06
0.02
0.00
Spawning Area
12 11 10 9 8 7 6 5 4 3 2 1
WEST
Nursery Area
EAST
WEST
EAST
0 0.3 0.6
Probability

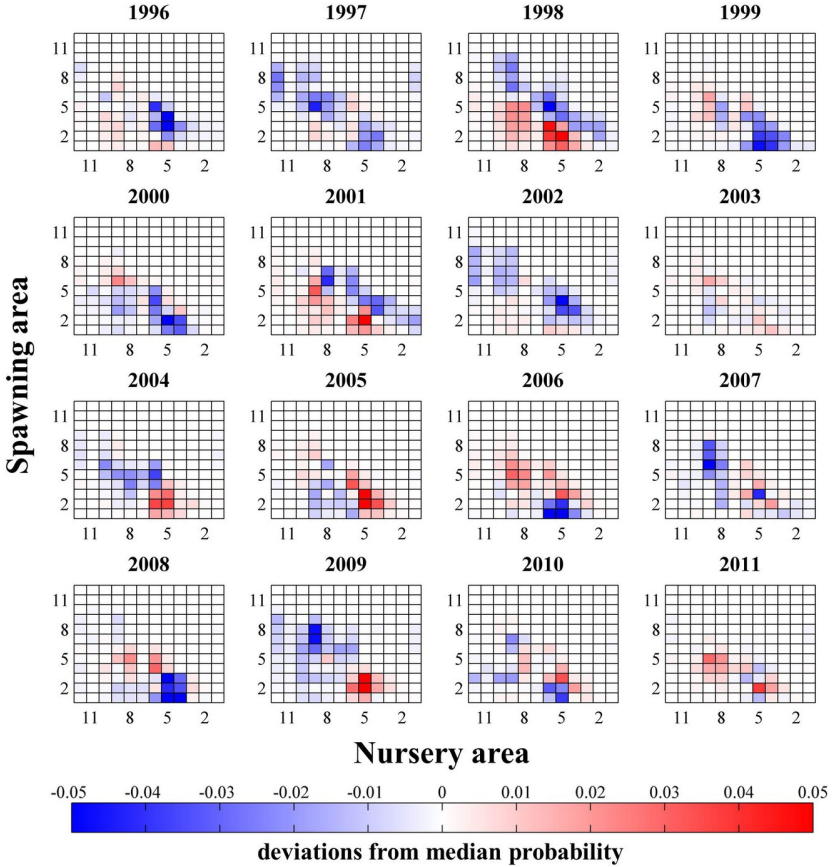
1996
1997
1998
1999
2000
2001
2002
2003
2004
2005
2006
2007
2008
2009
2010
2011
11
8
5
2
Spawning area
Nursery area
-0.05
-0.04
-0.03
-0.02
-0.01
0
0.01
0.02
0.03
0.04
0.05
deviations from median probability

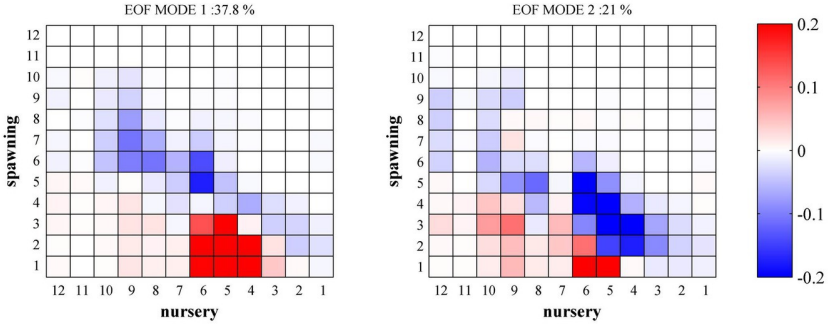
EOF MODE 1 :37.8 %
EOF MODE 2 :21 %
spawning
nursery
12 11 10 9 8 7 6 5 4 3 2 1
0.2
0.1
0
-0.1
-0.2

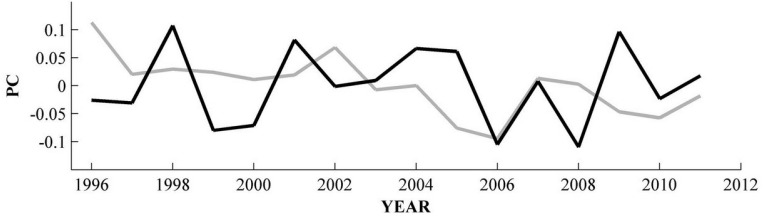
PC
YEAR
0.1
0.05
0
-0.05
-0.1
1996 1998 2000 2002 2004 2006 2008 2010 2012

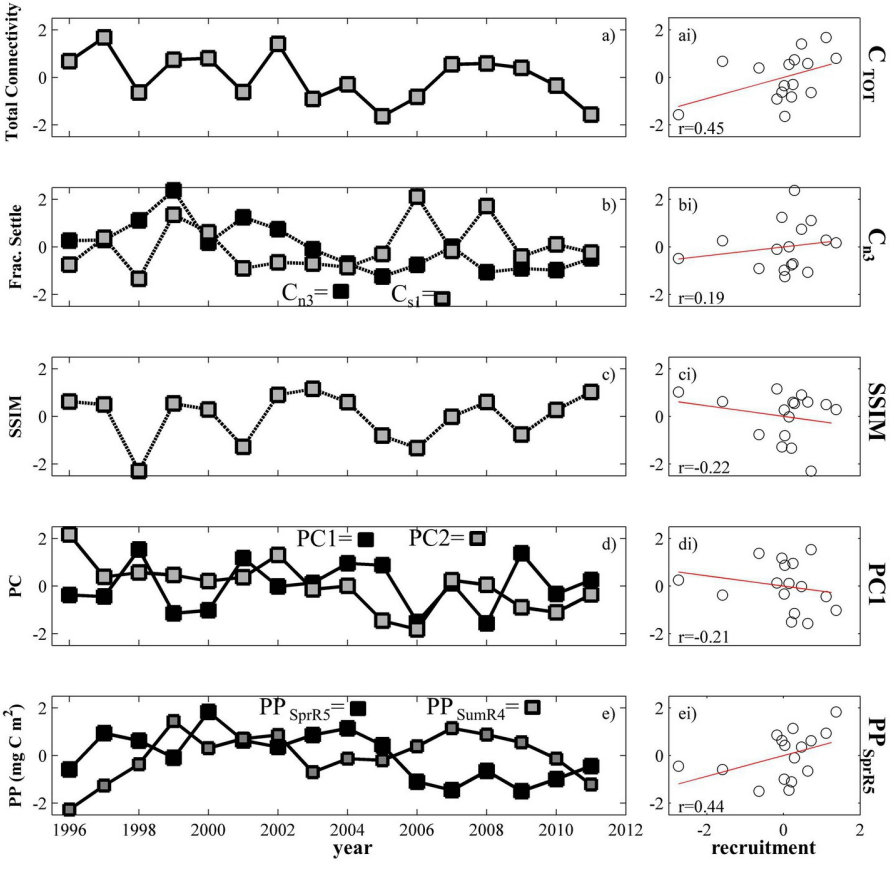
Total Connectivity
a)
ai)
C_{TOT}
r=0.45
Frac. Settle
b)
bi)
C_{n3}
C_{n3}=
C_{s1}=
r=0.19
SSIM
c)
ci)
SSIM
r=-0.22
PC
d)
di)
PC1
PC1=
PC2=
r=-0.21
PP (mg C m^2)
e)
ei)
PP_{SprR5}
PP_{SprR5}=
PP_{SumR4}=
r=0.44
1996
1998
2000
2002
2004
2006
2008
2010
2012
year
recruitment

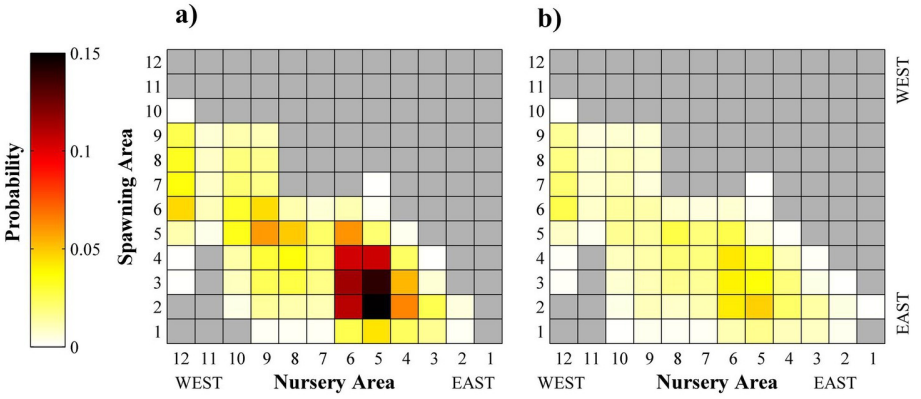
a)
b)
Probability
0.15
0.1
0.05
0
Spawning Area
12
11
10
9
8
7
6
5
4
3
2
1
WEST
EAST
Nursery Area

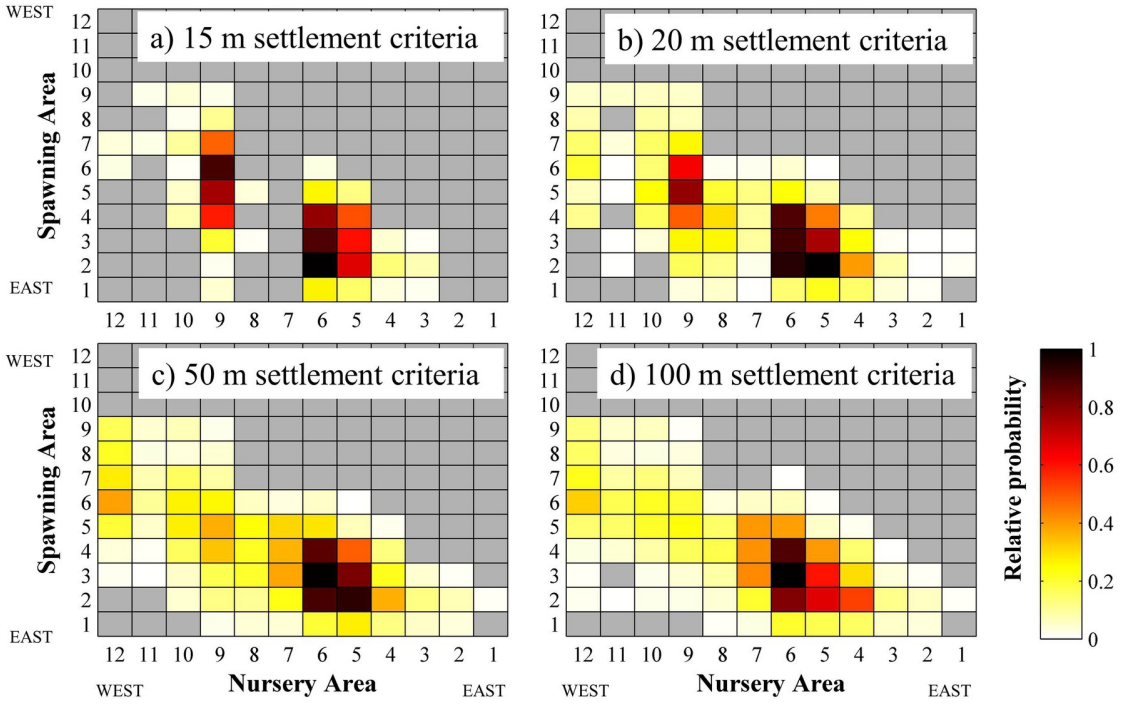
a) 15 m settlement criteria
b) 20 m settlement criteria
c) 50 m settlement criteria
d) 100 m settlement criteria
Spawning Area
Nursery Area
WEST
EAST
12 11 10 9 8 7 6 5 4 3 2 1
Relative probability
1
0.8
0.6
0.4
0.2
0

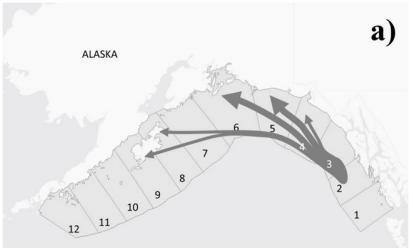
a)
ALASKA
6
5
4
3
2
1
7
8
9
10
11
12

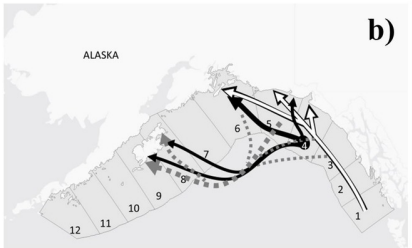
b)
ALASKA
6
5
4
3
2
1
7
8
9
10
11
12

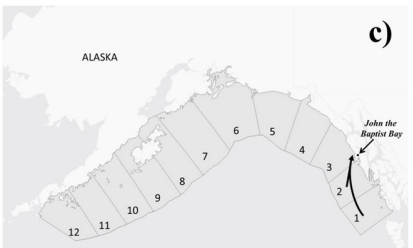
c)
ALASKA
John the Baptist Bay
6
5
4
3
2
1
7
8
9
10
11
12

Table 1. *Parameter values used in the sablefish IBM. The mode value was used in the baseline series of interannual runs for 1996-2011 and (unless an alternate number is presented in brackets) in conjunction with the minimum and maximum values (range), to define triangular probability distributions used in the parameter sensitivity analysis.*

Param.	Description	Mode	Range	Units	Source
Eggs (*E*)					
S_i	Initial Size	2	1.8-2.2	mm	[1]
g_E	Growth rate	0.28	0.097-0.294	mm/day	This study. Estimated from [2]
z_{minE}	Min. depth	213 (300)	240-360	m	[2,3,4,6]
z_{maxE}	Max. depth	360 (600)	480-720	m	[2,4,5,6]
v_E	Egg ascent rate	0.054	0.05-0.12	cm/s	This study. Approximated from [2]
d_{minE}	Min. stage duration	11.25	11-12	days	[2,4]
d_{maxE}	Max. stage duration	27	27-39	days	[2, 3]
ts_E	Min. size at hatching	5.35	4.7-6.0	mm	[2, 3]
Yolk Sac Larvae (*YSL*)					
g_Y	Growth rate	0.26	0.14-0.38	mm/day	Estimated – this study.
z_{minY}	Min. depth	500 (600)	500-800	m	[2,4]
z_{maxY}	Max. depth	1000	800-1000	m	[2,4,6]
v_Y	Vertical swim speed	0.143	0.078-29	cm/s	This study. Estimated from [2]
d_{minY}	Min. stage duration	7	7.0-11.6	days	[2]
d_{maxY}	Max. stage duration	20	19-40	days	[2, 4]
ts_Y	Min. size stage	7	7-8	mm	[2]
Feeding Larvae (*FL*)					
g_F	Growth rate	0.48	0.4-1.0	mm/day	Calculated from [3,7]
zd_{minF}	Min. day depth	0.25	0.0-0.5	m	[4]
zd_{maxF}	Max. day depth	0.75	0.5-1.0	m	[4]
v_F	Vertical swim speed	0.029	0.017-0.058	cm/s	Estimated from [4, Fig 4.]
d_{minF}	Min. stage duration	30	27-33	days	[17] Range is ± 10%
d_{maxF}	Max. stage duration	90	81-99	days	[17] Range is ± 10%
ts_F	Min. size at stage transition	35	31.5-38.5	mm	[3] Range is ± 10%
Epi-pelagic Juveniles (*EPJ*)					
g_P	Growth rate	1.8	0.9-2.24	mm/day	[3,8,9]
zd_{minP}	Min. depth	0.25	0.0-0.5	m	[3,10]
zd_{maxP}	Max. depth	0.75	0.5-1.0	m	[3]
v_P	Vertical swim speed	10	0.1-30	cm/s	Estimated from [11,12]
d_{minP}	Min. stage duration	11	9.9-12.1	days	Estimated from [9]. Range is ±10%

d_{maxP}	Max. stage duration	90	80-150	days	Estimated from [9]. Range is ±10%
ts_P	Min. size at stage transition	150	60-200	mm	[3,13,14]
Juveniles (*J*)					
g_J	Growth rate	1.47	0.90-2.24	mm/day	[9,13]
zd_{minJ}	Min. day depth	2	1-2	m	[12,15]
zd_{maxJ}	Max. day depth	20	2-20	m	Estimated from [12]
zn_{minJ}	Min. night depth	1	0-1	m	[12]
zn_{maxJ}	Max. night depth	10	1-10	m	[12]
v_J	Vertical swim speed	30	7.3-60	cm/s	Estimated from [11]
d_{maxJ}	Max. stage duration	∞ (90)	90-365	days	Estimated. This study.
h_s	Settlement depth	23.6	18.6-58.9	m	[16]

[1] Mason et al., 1983; [2] Alderdice et al., 1988; [3] Kendal and Matarese, 1987; [4] Mcfarlane and Beamish, 1992; [5] Moser et al., 1994; [6] McFarlane and Nagata, 1988; [7] Sogards 2011; [8] Shenker and Olla, 1986; [9] Boehlert and Yoklavich, 1985; [10] Doyle et al. 1994; [11] Ryer and Olla, 1997; [12] Sogard and Olla, 1998; [13] Sigleret al. 2001, [14] Shaw and McFariane, 1997; [15] Shenker, 1988, [16] Courtney and Rutecki, 2011; [17] This study: estimated from growth rate and transition sizes.

Table 2. Pearson's linear correlation coefficient as a measure of the degree of linear dependence between standardized recruitment and a suite of indices quantifying the environment (as predicted by ROMS model) and the connectivity of the spawning and nursery areas, as determined by the IBM. No mathematical correction was made for multiple comparisons. Correlations are rounded to two decimal places. Associated p-values are also reported, and correlations with a p-value < 0.1 are indicated with an asterisk.

Predictor	*Symbol*	*r*	*p*
Total Connectivity	C_{TOT}	0.45*	0.08
Structural Similarity Index	$SSIM$	-0.22	0.40
Structural component of SSIM	$SSIM_{str}$	-0.16	0.56
Luminescent component of SSIM	$SSIM_{lum}$	-0.19	0.47
Contrast component of SSIM	$SSIM_{con}$	-0.28	0.29
Fraction recruiting from spawning area 1	C_{s1}	0.26	0.33
Fraction recruiting to nursery area 3	C_{n3}	0.19	0.49
1st mode of EOF connectivity analysis	$PC1$	-0.21	0.43
2nd mode of EOF connectivity analysis	$PC2$	-0.03	0.92
Spring salinity anomaly eastern offshore region	$Salt_{SprR5}$	-0.11	0.68
Spring temperature anomaly eastern offshore region	$Temp_{SprR5}$	-0.25	0.35
Summer salinity anomaly eastern onshore region	$Salt_{SumR4}$	-0.08	0.76
Summer temperature anomaly eastern onshore region	$Temp_{SumR4}$	-0.04	0.87
Spring Primary Production eastern offshore region	PP_{SprR5}	0.44*	0.09
Summer Primary Production eastern onshore region	PP_{SumR4}	0.47*	0.07
Annual cross-shelf flow index 150-155°W (western Gulf)	$V_{X\,W}$	0.39*	0.15
Annual cross-shelf flow index 145-150°W (west-central Gulf)	$V_{X\,WC}$	0.56*	0.03
Annual cross-shelf flow index 140-145°W (east-central Gulf)	$V_{X\,EC}$	-0.09	0.74

Table 3. Results of ANOVA *to determine the variability in sablefish recruitment (R_s) that can be accounted for by variability in connectivity between spawning and nursery areas, and by primary production. To account for decreasing degrees of freedom in linear models including multiple predictors, adjusted R-squared (indicated by *) is reported rather than R-squared. The direction of the relationship between each predictor and recruitment are shown in Table 2.*

Predictors	Summary Statistics		
	R-squared	**F-statistic**	**p-value**
Total Connectivity	0.20	3.49	0.08
Spring Primary Production R5	0.19	3.29	0.09
Summer Primary Production R4	0.22	3.98	0.07
Annual cross-shelf flow (west-central Gulf)	0.26	5.97	0.03
Total Connectivity + *Spring Primary Production R5*	0.28*	3.88	0.05
Total Connectivity + *Summer Primary Production R4*	0.26*	3.61	0.06
Spring Primary Production R5 + *Summer Primary Production R4*	0.42*	6.39	0.01
Total Connectivity + *Annual cross-shelf flow (west-central Gulf)*	0.44	6.53	0.01
Total Connectivity + *Spring Primary Production R5* + *Summer Primary Production R4*	0.51*	6.12	0.01
Total Connectivity + *Annual cross-shelf flow (west-central Gulf)* + *Summer Primary Production R4*	0.45*	4.82	0.02
Total Connectivity + *Annual cross shelf flow (west-central Gulf)* + *Summer Primary Production R4* + *Spring Primary Production R5*	0.59*	5.99	0.01

Table 4. Top five ranked parameters for the four diagnostic variables considered. Refer to the Table 1 for parameter definitions.

	Variable			
Rank	C_{TOT}	C_{n3}	C_{s78}	$SSIM_{500}$
1st	h_s	h_s	h_s	ts_P
2nd	d_{maxJ}	ts_P	v_F	z_{maxE}
3rd	v_F	g_E	z_{minY}	zn_{minJ}
4th	zd_{minJ}	g_F	g_E	d_{minE}
5th	zn_{minJ}	v_F	zd_{maxJ}	d_{minP}

Table 5. R^2 values to indicate variability in the four output diagnostics that can be accounted for by variability in the top ten (Top_{10}), five (Top_5), and one (Top_4), ranked parameters, as defined in Table 2. Top_4 is the highest ranked four parameters once h_s habitat depth preference is removed. See Method section for description of sensitivity experiments.

	C_{TOT}	C_{n3}	C_{s78}	$SSIM_{500}$
Top_5	0.78	0.58	0.67	0.04
Top_{10}	0.79	0.60	0.69	0.05
Top_4*	0.06	0.13	0.24	0.01